

Maximum Principle of Optimal Probability Density Control

Nathan Gaby ^{*} Xiaojing Ye ^{†‡}

Abstract

We develop a general theoretical framework for optimal probability density control on standard measure spaces, aimed at addressing large-scale multi-agent control problems. In particular, we establish a maximum principle (MP) for control problems posed on infinite-dimensional spaces of probability distributions and control vector fields. We further derive the Hamilton–Jacobi–Bellman equation for the associated value functional defined on the space of probability distributions. Both results are presented in a concise form and supported by rigorous mathematical analysis, enabling efficient numerical treatment of these problems. Building on the proposed MP, we introduce a scalable numerical algorithm that leverages deep neural networks to handle high-dimensional settings. The effectiveness of the approach is demonstrated through several multi-agent control examples involving domain obstacles and inter-agent interactions.

Keywords: Control Hamiltonian dynamics, Hamilton–Jacobi–Bellman equation of value functional, Maximum principle, Optimal probability control.

1 Introduction

Optimal probability density control has recently gained significant attention due to its increasing prevalence in multi-agent control systems managing swarms of agents, such as drones, robots, and autonomous vehicles [9, 14, 18]. These problems are increasingly relevant in real-world applications, including large-scale surveillance, time-critical search-and-rescue operations, and infrastructure inspection.

Given the large scale of these systems, a probabilistic description of the state is often the most effective approach [25]. Consequently, a standard method for solving these multi-agent control problems is through mean-field modeling, which serves as a continuum approximation of the discrete multi-agent system. Here, the probability density of the agent states represents the entire system. Notably, the state of an agent may reside in a high-dimensional space, as it encompasses combined

^{*}Department of Mathematics and Computer Science, Berry College, Mount Berry, GA 30149, USA. (e-mail: ngaby1@berry.edu).

[†]Department of Mathematics and Statistics, Georgia State University, Atlanta, GA 30303, USA (e-mail: xye@gsu.edu).

[‡]This work is supported in part by National Science Foundation under grants DMS-2307466, DMS-2409868, and DMS-2510830.

variables such as location, orientation, velocity, and acceleration. In this regard, optimal probability control and multi-agent control are unified into the same problem framework, and the goal is to find the control vector field that maximizes a given total reward function describing the probability density, or equivalently the collective behaviors of the agents, with consideration of inter-agent collaboration and competitions.

Let Ω be an open subset of \mathbb{R}^d , where d is the dimension of state vector (such as the concatenation of location, orientation, acceleration, and etc.) of an agent. Suppose there are N agents with states $\{x_i \in \Omega : i = 1, \dots, N\}$ which follow some initial distribution p on Ω , i.e., $x_i \sim p$. Under a time-evolving control vector field $u : \Omega \times [0, T] \rightarrow \mathbb{R}^d$ over a fixed time horizon $[0, T]$, the states of the agents change according to

$$\dot{x}_i(t) = u(x_i(t), t), \quad i = 1, \dots, N. \quad (1)$$

Each agent accumulates some running rewards during $[0, T]$ and receives a terminal reward at time T . Unlike classical optimal control, these rewards *depend not only this specific agent but also the collective behaviors of all agents*. We provide a few examples of running and terminal reward functions below.

We use $\rho(\cdot, t)$ to denote the time marginal of the states $x_i(t)$ for every t , namely, $x_i(t) \sim \rho(\cdot, t)$. Then (1) corresponds to the continuity equation

$$\partial_t \rho(x, t) + \nabla \cdot (\rho(x, t) u(x, t)) = 0 \quad (2)$$

in $\Omega \times [0, T]$. For notation simplicity, we write $\rho(\cdot, t)$ and $u(\cdot, t)$ as ρ_t and u_t respectively, and often omit (x) in the integrals hereafter unless it is needed for clarification.

Consider for example that the agents are required to keep distances from each other to avoid collision. In this case, we can set the running reward received by the i th agent at time t as

$$-\frac{1}{2} |u(x_i(t), t)|^2 - \sum_{j \neq i} \frac{\gamma}{|x_j(t) - x_i(t)|^2 + \epsilon}, \quad (3)$$

where $\gamma, \epsilon > 0$ are user-selected hyperparameters. In (3), the first term penalizes the cost of control energy by the i th agent, whereas the second term penalizes the closeness to other agents, with γ as the penalty weight and ϵ a tiny threshold value ensuring the denominator is positive. Taking sum of (3) over $i = 1, \dots, N$, dividing by N , and letting $N \rightarrow \infty$, we find the continuum limit to be a functional of ρ_t and u_t :

$$-\frac{1}{2} \int_{\Omega} |u_t|^2 \rho_t dx - \int_{\Omega} \int_{\Omega} \frac{\gamma}{|y - x|^2 + \epsilon} \rho_t(y) \rho_t(x) dy dx. \quad (4)$$

This is an example of running reward functional $R(\rho_t, u_t)$.

For the terminal reward, a simple example is that we want all agents to gather at a specified state $x^* \in \Omega$ at the terminal time T . In this case, we can set the terminal reward received by the i th agent at T as

$$-\frac{1}{2} |x_i(T) - x^*|^2, \quad (5)$$

which encourages the i th agent to get close to the target x^* . Again, taking sum of $i = 1, \dots, N$, dividing by N , and letting $N \rightarrow \infty$, we obtain the total terminal reward functional of ρ_T :

$$-\frac{1}{2} \int_{\Omega} |x - x^*|^2 \rho_T(x) dx, \quad (6)$$

which is an example of terminal reward functional $G(\rho_T)$.

The running and terminal rewards (4) and (6) are typical examples in multi-agent control, whereas other suitable rewards can be designed according to specific applications.

Now we have the optimal probability control problem of interest in its general form as

$$\max_{u \in U_T} I[u] := \int_0^T R(\rho_t, u_t) dt + G(\rho_T), \quad (7a)$$

$$\text{s.t. } \partial_t \rho_t + \nabla \cdot (\rho_t u_t) = 0, \quad \forall (t, x) \in [0, T] \times \Omega, \quad (7b)$$

$$\rho_0 = p, \quad \forall x \in \Omega, \quad (7c)$$

where I is the total reward functional, U_T is the admissible set of control vector fields, and p is a given initial probability distribution, i.e., $x_i(0) \sim p$. (We assume $I^* := \max_{u \in U_T} I[u]$ to be finite in this work.) We will give the definitions of the terms in (7) in detail in Section 3.

The main goal of this work is to establish a maximum principle of the optimal probability control problem (7) in Section 3.1, along with newly defined adjoint partial differential equation (adjoint PDE) and control Hamiltonian functional H . In addition to the maximum principle, we establish the Hamilton–Jacobi–Bellman equation of the value functional associated with (7) in Section 3.2. Moreover, we develop a numerical algorithm aligned with the proposed maximum principle and demonstrate its performance on several probability (multi-agent) control examples in Section 4.

The novelty and significance of the results presented in this work are in two phases: (i) These results are rigorously established on the infinite-dimensional space of probability density functions in contrast to finite-dimensional Euclidean space in classic control theory; and (ii) Our theory is built on standard measure space, yielding concise presentation, simple interpretation, and developments of fast numerical algorithms for applications.

2 Related Work

Characterizing behaviors of large multi-agent systems using probability distributions is typically called a mean-field model. The approach of mean-field model to approximating multi-agent system can be traced back to [29]. Theoretical justifications are provided in [19, 20]. Mean-field models are also used to establish Nash equilibrium in the case where each agent try to maximal its individual reward depending on the configurations of all the other agents in large multi-agent systems. This is an important research topic, known as the mean field game (MFG) [11, 27, 30], which has been intensively studied in the past two decades.

In this section, we present an overview of optimality conditions and numerical algorithms for general probability control problem (7). Due to space limitation, we omit results for special cases of (7), such as those with control-affine drifts and quadratic running cost.

A substantial body of theoretical studies on optimality conditions of probability control has been developed in the Wasserstein space of probability measures, grounded in optimal transport theory [1, 3, 36, 37]. In [6, 7, 8], a series of studies are conducted on the Pontryagin maximum principle (PMP) of probability control problems on the Wasserstein space, where the optimality condition is formulated using the Wasserstein subdifferential [1, 2] and the Hamiltonian, forward-backward continuity equation, and the PMP are defined on the joint probability with one of the two marginals being the probability to be controlled. In [4], the optimality conditions for the probability control problem on Wasserstein space are established from the mean-field approach with a coupled

ODE-PDE constraint. In [25], the value function is proved to be the unique viscosity solution of a first-order Hamilton–Jacobi–Bellman equation under mild regularity conditions in the Wasserstein space. Such result is also extended to Mayer-type optimal control problems on the Wasserstein space defined over compact Riemannian manifold in [24]. The conditions for approximate and exact controllability where control is restricted to a local bounded region are investigated in [16], which also rely on the theory of Wasserstein spaces such as Wasserstein subdifferential.

By contrast, the present work follows an alternative approach to (7) which does not involve Wasserstein spaces and metrics. The derivations are established on basic measurable spaces and metrics in analysis, such as L^2 space and metric, yielding concise presentation and simple computations. This is the main difference between this work and the aforementioned ones in the literature.

This work is partly motivated by the limited existing results on fast numerical methods for solving the optimal probability control (7), particularly for high-dimensional problems. Existing works in this field are mostly concerned about approximating a given target distribution from an initial one without any cost or reward of the time-dependent control vector field. For instance, in [17], the control field is determined by the difference between the current and target densities, which must be known with explicit forms, and is proved to achieve the density matching goal. In [33], a numerical method for solving the optimal probability control problem with particle randomness, for which the continuity equation is replaced with a Fokker–Planck equation, is considered. In [35], the control function is approximated with one-dimensional radial basis functions, the PDEs of the state and adjoint are discretized in space with finite element method, and the integral in time is approximated by the trapezoidal method. Using Wasserstein-2 distance between the current probability, which is represented by the average of Dirac delta functions at the current particle locations, and the target probability is used as the running cost, numerical experiments conducted on one- and two-dimensional cases are presented in [23]. In [31], a numerical method is developed to solve a special probability control problem with continuity equation, where the goal is to maximize the density mass in a target region at terminal time. The method is not applicable to general probability control problems and the numerical experiments are mostly conducted in two-dimensional cases. In [10], the PMP is applied to optimal control problems governed by the Fokker–Planck equation, and a finite difference scheme based on the sequential quadratic Hamiltonian (SQH) method is developed for low-dimensional problems. The work [21] considers the Mayer-type optimal probability control problem where the Wasserstein distance between the final probability and the target probability as a terminal cost. It is a discrete-time version where at each time the state is pushed forward by a control to be solved, and the control is obtained by employing normalizing flows [13] to minimize the terminal cost. Several numerical examples are provided for two-dimensional problems. In [22], an extended version to the case where the dynamics is described by a stochastic differential equation is considered, where maximum principle is established on the state and adjoint variables, not on the probability density and adjoint function, and no numerical result is provided. The optimal probability control problem with Wasserstein-1 distance between the target density and controlled density at terminal time as the terminal cost is considered in [28], where Wasserstein-1 distance is reformulated in its dual form and the control problem reduces to a minimax problem. The control vector field is parameterized as a deep neural network and experiments are performed on a few high-dimensional problems. However, these methods are not applicable to high-dimensional problems due to spatial discretizations or lack control-theoretic guarantees for solution optimality.

3 Theory of Optimal Probability Control

In this section, we develop the maximum principle and the Hamilton–Jacobi–Bellman (HJB) equation for the optimal probability control problem (7). They are analogues to the Pontryagin maximum principle and HJB equation in classical optimal control. The difference is that the ones introduced in this work are defined on the space of probability density functions, instead of finite-dimensional Euclidean spaces.

In the remainder of this paper, we use $|\cdot|$ to denote the absolute value of scalars and 2-norm of vectors, and $a \cdot b$ as the inner product of two vectors a and b . For the $L^2(\Omega)$ space, we use $\|\cdot\|_2$ and $\langle \cdot, \cdot \rangle$ to denote its associated norm and inner product, respectively. We use ∇ to denote the gradient (Jacobian) of a scalar-valued (vector-valued) function with respect to x , $\nabla \cdot$ is the divergence, and ∂_* and ∇_* for partial and full gradient with respect to the variable at the place of $*$, respectively. Furthermore, $\frac{\delta}{\delta \rho} G(\rho)$ is the Fréchet derivative of a functional G with respect to its variable ρ in the L^2 sense.

We define the space of probability density functions on Ω :

$$P = \left\{ p : \Omega \rightarrow [0, \infty) : \int_{\Omega} p(x) dx = 1 \right\}. \quad (8)$$

Furthermore, for the given terminal time $T > 0$, we define the space of time-evolving probability density functions as:

$$P_T = \left\{ \rho : \Omega \times [0, T] \rightarrow \mathbb{R} : \rho(\cdot, t) \in P, \forall t \in [0, T] \right\},$$

We assume that the admissible set of control vector field at any fixed time is

$$U = \left\{ w \in C(\bar{\Omega}; \mathbb{R}^d) : \text{Lip}(w) \leq M_U, (w \cdot n)|_{\partial\Omega} = 0 \right\}, \quad (9)$$

for some $M_U > 0$, namely, w is M_U -Lipschitz continuous in $\bar{\Omega}$ and satisfies the boundary condition $w(x) \cdot n(x) = 0$, where $n(x) \in \mathbb{R}^d$ is the outer normal of $\partial\Omega$ at x for all $x \in \partial\Omega$. The boundary condition of w conserves the total probability density as 1. Then we define the admissible set of time-evolving control vector fields as

$$U_T = \left\{ u : \bar{\Omega} \times [0, T] \rightarrow \mathbb{R}^d : u(\cdot, t) \in U, \forall t \in [0, T] \right\}. \quad (10)$$

Note that (10) does not require $u(x, \cdot)$ to be a continuous function of t , allowing u to change direction instantaneously and yielding broader range of applications of the results obtained in this work.

We have a few assumptions on the probability distributions and controls as follows, which ensure the derivations later can be carried out rigorously.

Assumption 3.1. *We make the following assumptions:*

- (i) For all $x \in \Omega$, $\rho(x, \cdot)$ is differentiable in t on $[0, T]$.
- (ii) For all $t \in [0, T]$, $\rho(\cdot, t)u(\cdot, t)$ is differentiable in Ω .
- (iii) For all $x \in \Omega$, $\rho(x, \cdot)u(x, \cdot)$ has Lebesgue points in $(0, T)$ everywhere.
- (iv) For all $w \in U$, $R(\cdot, w)$ is Fréchet differentiable in P in the L^2 sense.

(v) $G(\cdot)$ is Fréchet differentiable in P in the L^2 sense.

Assumption 3.1 (i) and (ii) can be relaxed to weakly differentiable as long as (2) is valid. Assumption 3.1 (iii) ensures $\frac{d}{dt} \int_0^t \rho(x, s)u(x, s) ds = \rho(x, t)u(x, t)$ for all $t \in (0, T)$. This is used in a step in the proof of Lemma 3.7 below (we will specify it in the proof). Assumption 3.1 (iv) and (v) allow functional derivatives of R and G at any $p \in P$, which are needed in the establishment of control Hamiltonian dynamics later. Notice that running and terminal reward functionals in real-world applications typically satisfy Assumption 3.1 (iv) and (v). For example, the running reward in (4) has functional derivative

$$\frac{\delta}{\delta \rho_t} R(\rho_t, u_t)(x) = -\frac{1}{2}|u_t(x)|^2 - \int_{\Omega} \frac{\gamma \rho_t(y)}{|y-x|^2 + \epsilon} dy$$

and the terminal reward in (6) has functional derivative

$$\frac{\delta}{\delta \rho_T} G(\rho_T)(x) = -\frac{1}{2}|x - x^*|^2.$$

We will show experimental results on (7) with other running and terminal reward functionals in Section 5.

3.1 Maximum Principle for Probability Control

We establish a maximum principle (MP) for the optimal probability control problem (7) with any initial value $p \in P$ in this subsection. As an analogue to the Pontryagin MP for classic optimal control, our MP is a time pointwise necessary condition of the optimal solution u to (7) defined on the infinite-dimensional spaces P_T and U_T . To develop our MP, we first introduce the definition of adjoint partial differential equation (PDE) and control Hamiltonian functional.

Definition 3.2 (Adjoint PDE). *Let $u \in U_T$ be a control vector field and $\rho \in P_T$ the corresponding evolutionary probability function solving (7b) with initial (7c). Define an evolution PDE by*

$$\partial_t \phi_t + u_t \cdot \nabla \phi_t = -\frac{\delta}{\delta \rho_t} R(\rho_t, u_t) \tag{11}$$

in $\Omega \times [0, T]$. We call (11) the adjoint PDE associated to (ρ, u) . We call ϕ the adjoint function of (ρ, u) if $\phi : \Omega \times [0, T] \rightarrow \mathbb{R}$ solves (11) with terminal condition $\phi_T = \frac{\delta}{\delta \rho_T} G(\rho_T)$.

Throughout this work, we assume $\frac{\delta}{\delta \rho} R(\cdot, w)$, $\frac{\delta}{\delta \rho} G(\cdot)$, and u in the control problem (7) are sufficiently smooth for any $w \in U$ such that the following assumption holds.

Assumption 3.3. *An adjoint function $\phi : \Omega \times [0, T] \rightarrow \mathbb{R}$ for (7) with any initial $p \in P$ exists.*

We see that Assumption 3.3 holds for typical application problems, such as those with the running and terminal reward functionals defined in (4) and (6).

Note that the adjoint function ϕ has spatial variable x and time variable t , and the adjoint equation is an evolution PDE. By contrast, in classical optimal control, the adjoint function is a function of t only, and the adjoint equation is an ODE.

Definition 3.4 (Hamiltonian functional). *Let $p \in P$, $w \in U$, and $f : \Omega \rightarrow \mathbb{R}$ be a differentiable function, we define the Hamiltonian functional by*

$$H(p, f, w) = \langle p, w \cdot \nabla f \rangle + R(p, w). \quad (12)$$

where R is the running reward functional in (7).

Now we can verify that (ρ, ϕ) induced by any $u \in U_T$ satisfies the symplectic control Hamiltonian dynamics, as summarized in the following proposition.

Proposition 3.5 (Control Hamiltonian dynamics). *Let $u \in U_T$ be a control vector field, $\rho \in P_T$ the corresponding evolutionary probability, and ϕ the adjoint function of (ρ, u) . Then (ρ, ϕ) satisfies the control Hamiltonian dynamics:*

$$\begin{cases} \partial_t \rho_t = \frac{\delta}{\delta \phi_t} H(\rho_t, \phi_t, u_t) = -\nabla \cdot (\rho_t u_t), \\ \partial_t \phi_t = -\frac{\delta}{\delta \rho_t} H(\rho_t, \phi_t, u_t) = -u_t \cdot \nabla \phi_t - \frac{\delta}{\delta \rho_t} R(\rho_t, u_t) \end{cases} \quad (13)$$

for all t .

The dynamics (13) are easy to verify using (2), (11), and (12), and hence we omit the proof of Proposition 3.5.

In what follows, we write u^* as an optimal control vector field of (7) and ρ^* the corresponding probability. Then we define a needle-like variant u^ϵ of u^* as follows: For any time $\tau \in (0, T)$ and $\epsilon \in (0, \tau)$, and $w \in U$, we define

$$u_t^\epsilon := \begin{cases} w, & \tau - \epsilon < t \leq \tau, \\ u_t^*, & \text{otherwise.} \end{cases} \quad (14)$$

We denote by $\rho_t^\epsilon \in P_T$ the evolutionary probability determined by (2) with control vector field set to $u^\epsilon \in U_T$ and initial $\rho_0^\epsilon = p$. Next, we introduce the perturbation function that describes the first-order approximation of ρ_t^ϵ to ρ_t .

Definition 3.6 (Perturbation function). *For any $\tau \in (0, T)$, we define the function $\sigma : [0, T] \times \Omega \rightarrow \mathbb{R}$ as follows: If $t \in [0, \tau)$, then*

$$\sigma_t = 0; \quad (15)$$

If $t \in [\tau, T]$, then σ is defined as the solution to the initial value problem:

$$\begin{cases} \partial_t \sigma_t = -\nabla \cdot (u_t^* \sigma_t), & \forall t > \tau, \\ \sigma_\tau = -\nabla \cdot (\rho_\tau^* (w - u_\tau^*)). \end{cases} \quad (16)$$

Note that $\sigma_t(x)$ is not necessarily differentiable at $t = \tau$ for a fixed x , and σ_t depends on τ and w but not ϵ . We show that the first-order approximation of ρ_t^ϵ to ρ_t is σ_t in the following lemma.

Lemma 3.7. *Suppose $\tau \in (0, T)$, $\epsilon \in (0, \tau)$, $w \in U$, and u_t^ϵ is defined in (14). Let σ_t be the perturbation function in Definition 3.6. Then for every $t \in [0, T]$, there is*

$$\lim_{\epsilon \rightarrow 0} \frac{1}{\epsilon} \|\rho_t^\epsilon - \rho_t^* - \epsilon \sigma_t\|_2 = 0. \quad (17)$$

Proof. We prove (17) in three cases: $t \in [0, \tau)$, $t = \tau$, and $t \in (\tau, T]$.

For any $t \in [0, \tau)$, let $\epsilon \in (0, \tau - t)$, then there is $t < \tau - \epsilon$. By (15), we know $\sigma_t = 0$. By (14), we have $\rho_s^\epsilon = \rho_s^*$ for all $s < \tau - \epsilon$. Therefore $\rho_t^\epsilon = \rho_t^*$.

For $t = \tau$, we only need to show that σ_τ defined by the initial condition in (16) is equal to $\lim_{\epsilon \rightarrow 0} \frac{\rho_\tau^\epsilon - \rho_\tau^*}{\epsilon}$ almost everywhere in Ω . To this end, let $\psi \in H_0^1(\Omega)$ be arbitrary, then there is

$$\begin{aligned}
\int_{\Omega} \left(\lim_{\epsilon \rightarrow 0} \frac{\rho_\tau^\epsilon - \rho_\tau^*}{\epsilon} \right) \psi \, dx &= \lim_{\epsilon \rightarrow 0} \frac{1}{\epsilon} \int_{\Omega} (\rho_\tau^\epsilon - \rho_\tau^*) \psi \, dx \\
&= \lim_{\epsilon \rightarrow 0} \frac{1}{\epsilon} \int_{\Omega} \left(\int_{\tau-\epsilon}^{\tau} (\partial_s \rho_s^\epsilon - \partial_s \rho_s^*) \, ds \right) \psi \, dx \\
&= \lim_{\epsilon \rightarrow 0} \frac{1}{\epsilon} \int_{\tau-\epsilon}^{\tau} \int_{\Omega} (w \rho_s^\epsilon - u_s^* \rho_s^*) \cdot \nabla \psi \, dx \, ds \\
&= \int_{\Omega} \left(\lim_{\epsilon \rightarrow 0} \frac{1}{\epsilon} \int_{\tau-\epsilon}^{\tau} (w - u_s^*) \rho_s^* \, ds \right) \cdot \nabla \psi \, dx \\
&= \int_{\Omega} (w - u_\tau^*) \rho_\tau^* \cdot \nabla \psi \, dx \\
&= - \int_{\Omega} \nabla \cdot ((w - u_\tau^*) \rho_\tau^*) \psi \, dx \\
&= \int_{\Omega} \sigma_\tau \psi \, dx
\end{aligned} \tag{18}$$

where the first equality of (18) is due to the Lebesgue dominated convergence theorem; the second due to $\rho_{\tau-\epsilon}^\epsilon = \rho_{\tau-\epsilon}^*$ and integration in time; the third by the continuity equations of ρ^ϵ and ρ^* , integration by parts on Ω , and $w, u_\tau^* \in U$ (so that $(w \cdot n)|_{\partial\Omega} = 0$ and $(u_\tau^* \cdot n)|_{\partial\Omega} = 0$); the fourth by the Lebesgue dominated convergence theorem; the fifth by Assumption 3.1 (iii); the sixth is due to integration by parts and $w, u_\tau^* \in U$; and the last equality by the initial condition in (16).

For $t > \tau$, define $\delta(t) := \frac{1}{2} \|\rho_t^\epsilon - \rho_t^* - \epsilon \sigma_t\|_2^2$, then there is

$$\begin{aligned}
\dot{\delta}(t) &= \int_{\Omega} (\rho_t^\epsilon - \rho_t^* - \epsilon \sigma_t) \partial_t (\rho_t^\epsilon - \rho_t^* - \epsilon \sigma_t) \, dx \\
&= - \int_{\Omega} (\rho_t^\epsilon - \rho_t^* - \epsilon \sigma_t) \nabla \cdot (u_t^* (\rho_t^\epsilon - \rho_t^* - \epsilon \sigma_t)) \, dx \\
&= \int_{\Omega} u_t^* \cdot \nabla \left(\frac{1}{2} |\rho_t^\epsilon - \rho_t^* - \epsilon \sigma_t|^2 \right) \, dx \\
&\leq dM_U \delta(t),
\end{aligned} \tag{19}$$

where the second equality is due to the continuity equations of ρ_t^ϵ , ρ_t^* and σ_t on $(\tau, T]$; the third is due to integration by parts and $(u_t^* \cdot n)|_{\partial\Omega} = 0$; and the last equality is due to $\text{Lip}(u_t) \leq M_U$ yielding $\|\nabla \cdot u_t^*\|_\infty \leq dM_U$. By Grönwall's inequality, we have $\delta(t) \leq \delta(\tau) e^{dM_U(T-t)} \leq \delta(\tau) e^{dM_U T}$ for all $t \in (\tau, T]$. As we have shown that (17) holds true at $t = \tau$, namely, $\delta(\tau) = o(\epsilon^2)$, we obtain $\delta(t) = o(\epsilon^2)$, which implies (17) for all $t \in (\tau, T]$. \square

In the next lemma, we derive the first variation of I , which is critical in the proof of the maximum principle that leverages the optimality of u^* .

Lemma 3.8. Let u^ϵ be defined in (14) and I defined in (7) with control vector field u^ϵ , then

$$\frac{d}{d\epsilon} I[u^\epsilon] \Big|_{\epsilon=0} = R(\rho_s^*, w) - R(\rho_s^*, u_s^*) + \left\langle \frac{\delta}{\delta \rho_T^*} G(\rho_T^*), \sigma_T \right\rangle + \int_0^T \left\langle \frac{\delta}{\delta \rho_t^*} R(\rho_t^*, u_t^*), \sigma_t \right\rangle dt$$

where σ_t is given in Definition 3.6.

Proof. First of all, we have

$$I[u^\epsilon] = \int_0^{\tau-\epsilon} R(\rho_t^\epsilon, u_t^*) dt + \int_{\tau-\epsilon}^\tau R(\rho_t^\epsilon, w) dt + \int_\tau^T R(\rho_t^\epsilon, u_t^*) dt + G(\rho_T^\epsilon). \quad (20)$$

Differentiating with respect to ϵ , using Lemma 3.7, and setting $\epsilon = 0$, we find that

$$\begin{aligned} \frac{d}{d\epsilon} I[u^\epsilon] \Big|_{\epsilon=0} &= \int_0^\tau \left\langle \frac{\delta}{\delta \rho_t^*} R(\rho_t^*, u_t^*), \sigma_t \right\rangle dt - R(\rho_\tau^*, u_\tau^*) + R(\rho_\tau^*, w) \\ &\quad + \int_\tau^T \left\langle \frac{\delta}{\delta \rho_t^*} R(\rho_t^*, u_t^*), \sigma_t \right\rangle dt + \left\langle \frac{\delta}{\delta \rho_T^*} G(\rho_T^*), \sigma_T \right\rangle \\ &= R(\rho_\tau^*, w) - R(\rho_\tau^*, u_\tau^*) + \int_0^\tau \left\langle \frac{\delta}{\delta \rho_t^*} R(\rho_t^*, u_t^*), \sigma_t \right\rangle dt + \left\langle \frac{\delta}{\delta \rho_T^*} G(\rho_T^*), \sigma_T \right\rangle, \end{aligned}$$

which completes the proof. \square

Now we are ready to establish the maximum principle which provides a time pointwise necessary condition of any optimal control vector field u^* .

Theorem 3.9 (Maximum Principle). Let u^* be an optimal solution to (7) with corresponding density ρ^* and ϕ^* the adjoint function of (ρ^*, u^*) . Then (ρ^*, ϕ^*, u^*) satisfies the control Hamiltonian dynamics (13) with $\rho_0^* = p$ and $\phi_T^* = \frac{\delta}{\delta \rho_T} G(\rho_T)$, and the following holds for all $\tau \in [0, T]$:

$$H(\rho_\tau^*, \phi_\tau^*, u_\tau^*) = \max_{w \in U} H(\rho_\tau^*, \phi_\tau^*, w). \quad (21)$$

Proof. Let $\tau \in [0, T]$ and $w \in U$ and define u^ϵ as in (14) with τ and w . Noting that u^* is optimal for (7) and applying Lemma 3.8, we find

$$0 \geq \frac{d}{d\epsilon} I[u^\epsilon] \Big|_{\epsilon=0} = R(\rho_\tau^*, w) - R(\rho_\tau^*, u_\tau^*) + \left\langle \frac{\delta}{\delta \rho_T^*} G(\rho_T^*), \sigma_T \right\rangle + \int_0^T \left\langle \frac{\delta}{\delta \rho_t^*} R(\rho_t^*, u_t^*), \sigma_t \right\rangle dt. \quad (22)$$

On the other hand, we have

$$\langle \phi_T^*, \sigma_T \rangle = \langle \phi_\tau^*, \sigma_\tau \rangle + \int_\tau^T \left(\langle \partial_t \phi_t^*, \sigma_t \rangle + \langle \phi_t^*, \partial_t \sigma_t \rangle \right) dt. \quad (23)$$

Substituting the adjoint PDE (11) for (ρ^*, u^*) and the conditions (16) for σ into (23), and integrating by parts, we obtain

$$\begin{aligned} \langle \phi_T^*, \sigma_T \rangle &= \langle \phi_\tau^*, \sigma_\tau \rangle - \int_\tau^T \left\langle \frac{\delta}{\delta \rho_t^*} R(\rho_t^*, u_t^*), \sigma_t \right\rangle dt \\ &= \langle \phi_\tau^*, \sigma_\tau \rangle - \int_0^T \left\langle \frac{\delta}{\delta \rho_t^*} R(\rho_t^*, u_t^*), \sigma_t \right\rangle dt, \end{aligned} \quad (24)$$

where the second equality is due to $\sigma_t = 0$ for all $t \in [0, \tau)$.

We combine (22) and (24) as well as the terminal condition $\phi_T^* = \frac{\delta}{\delta \rho_T^*} G(\rho_T^*)$ to conclude

$$0 \geq R(\rho_\tau^*, w) - R(\rho_\tau^*, u_\tau^*) + \langle \phi_\tau^*, \sigma_\tau \rangle. \quad (25)$$

On the other hand, we have

$$\begin{aligned} \langle \phi_\tau^*, \sigma_\tau \rangle &= \langle \phi_\tau^*, -\nabla \cdot (w - u_\tau^*) \rho_\tau^* \rangle \\ &= \langle u_\tau^* \cdot \nabla \phi_\tau^*, \rho_\tau^* \rangle - \langle w \cdot \nabla \phi_\tau^*, \rho_\tau^* \rangle, \end{aligned} \quad (26)$$

where the first equality is due to the value of σ_τ in the initial condition in (16), and the last equality is due to integration by parts. Combining (25) and (26), we have

$$\begin{aligned} 0 &\geq (R(\rho_\tau^*, w) + \langle u_\tau^* \cdot \nabla \phi_\tau^*, \rho_\tau^* \rangle) - (R(\rho_\tau^*, u_\tau^*) + \langle w \cdot \nabla \phi_\tau^*, \rho_\tau^* \rangle) \\ &= H(\rho_\tau^*, \phi_\tau^*, w) - H(\rho_\tau^*, \phi_\tau^*, u_\tau^*). \end{aligned}$$

As this is true for each $\tau \in [0, T]$ and $w, u_\tau^* \in U$, the claim (21) is proved. \square

Example 3.10. Let $T > 0$ be arbitrary and fixed, and $\Omega = \mathbb{R}^d$. Consider the control problem (7) with running reward

$$R(\rho_t, u_t) = -\frac{1}{2} \int_{\Omega} |u_t(x)|^2 \rho_t(x) dx \quad (27)$$

and terminal reward

$$G(\rho_T) = -\frac{1}{2} \int_{\Omega} |x|^2 \rho_T(x) dx. \quad (28)$$

We can choose any positive $p \in P$, namely $p(x) > 0$ for all $x \in \Omega$, as the initial ρ_0 in (7).

We can set the terminal reward (28) to $G(\rho_T) = -\frac{1}{2} \int_{\Omega} |x - x^*|^2 \rho_T(x) dx$ for any x^* , and the calculations below are similar. We use $x^* = 0$ for simplicity here.

By Definition 3.4, the Hamiltonian functional is

$$H(\rho_t, \phi_t, u_t) = \langle \rho_t, u_t \cdot \nabla \phi_t \rangle - \frac{1}{2} \int_{\Omega} |u_t|^2 \rho_t dx. \quad (29)$$

From (13), we have the control Hamiltonian dynamics of (ρ, ϕ) as

$$\begin{cases} \partial_t \rho_t = -\nabla \cdot (\rho_t u_t), \\ \partial_t \phi_t = -u_t \cdot \nabla \phi_t + \frac{1}{2} |u_t|^2, \end{cases} \quad (30)$$

with initial value of ρ as

$$\rho_0 = p \quad (31)$$

and terminal value of ϕ as

$$\phi_T = \frac{\delta}{\delta \rho_T} G(\rho_T) = -\frac{1}{2} |x|^2. \quad (32)$$

By the maximum principle (21), there is

$$\begin{aligned} H(\rho_t, \phi_t, u_t) &= \max_{w \in U} H(\rho_t, \phi_t, w) \\ &= \max_{w \in U} \left\{ \langle \rho_t, w \cdot \nabla \phi_t \rangle - \frac{1}{2} \int_{\Omega} |w|^2 \rho_t dx \right\}. \end{aligned} \quad (33)$$

Completing the square in the maximization above, we deduce that the maximizer u_t satisfies $\rho_t(u_t - \nabla\phi_t) = 0$. Assuming $\rho_t > 0$, we have

$$u_t = \nabla\phi_t. \quad (34)$$

Plugging (34) into the control Hamiltonian dynamics (30), and combining with (31) and (32), we know that the optimal ρ solves the initial value problem

$$\begin{cases} \partial_t \rho_t + \nabla \cdot (\rho_t \nabla \phi_t) = 0, & \forall t \in [0, T], \\ \rho_0 = p, \end{cases} \quad (35)$$

and its corresponding adjoint function ϕ solves the terminal value problem

$$\begin{cases} \partial_t \phi_t + \frac{1}{2} |\nabla \phi_t|^2 = 0, & \forall t \in [0, T], \\ \phi_T = -\frac{1}{2} |x|^2. \end{cases} \quad (36)$$

We can verify that the solution to (36) is

$$\phi_t(x) = \frac{|x|^2}{2(t - T - 1)}. \quad (37)$$

This implies that the optimal control vector field is

$$u_t(x) = \frac{x}{t - T - 1} \quad (38)$$

for all x and t . We will continue with this example to see its value functional and HJB equation in the next subsection.

3.2 HJB Equation for Probability Control

In this subsection, we derive the Hamilton–Jacobi–Bellman (HJB) equation associated with the optimal probability control problem (7). To this end, we need to define value functional, which is an analogue to the value function in the classic optimal control. Note that this is a time-evolving functional defined on the cross space $P \times [0, T]$. The definition of this value functional is as follows.

Definition 3.11 (Value functional). *For any $p \in P$ and $t \in [0, T]$, define the time-evolving functional V by*

$$V(p, t) = \sup_{u \in \bar{U}_T} \left\{ \int_t^T R(\rho_s, u_s) ds + G(\rho_T) \right\} \quad (39)$$

where ρ_s solves the initial value problem:

$$\begin{cases} \partial_s \rho_s + \nabla \cdot (u_s \rho_s) = 0, & \forall s \in [t, T], \\ \rho_t = p. \end{cases} \quad (40)$$

We call H the value functional of (7).

Note that, for any t , $V(\cdot, t) : P \rightarrow \mathbb{R}$ is a functional on the infinite-dimensional space of probability density functions on Ω . By contrast, value function in classical optimal control is function on some subset of finite-dimensional Euclidean space.

Now we are ready to establish the HJB equation of the value functional V as follows.

Theorem 3.12 (HJB equation for probability control). *If $V(\cdot, t)$ is continuously Fréchet differentiable in P for all t and $V(p, \cdot)$ is C^1 in $[0, T]$ for all $p \in P$, then $V : [0, T] \times P \rightarrow \mathbb{R}$ satisfies*

$$\partial_t V(p, t) + \max_{w \in U} \left\{ \left\langle w \cdot \nabla \frac{\delta}{\delta p} V(p, t), p \right\rangle + R(p, w) \right\} = 0, \quad (41)$$

with terminal value $V(\cdot, T) = G(\cdot)$ in Ω .

Proof. It is clear that $V(p, T) = G(p)$ for any $p \in P$ by (39) and (40). Now let $p \in P$, $t \in [0, T]$. For any $\epsilon > 0$, we consider the constant control $w \in U$ in the interval $[t, t + \epsilon] \subset [0, T]$ and the associated evolution ρ_s given by

$$\begin{cases} \partial_s \rho_s(x) + \nabla \cdot (w \rho_s) = 0, & \forall s \in (t, t + \epsilon), \\ \rho_t = p. \end{cases}$$

From the definition of the value functional (39), we know

$$V(p, t) \geq \int_t^{t+\epsilon} R(\rho_s, w) ds + V(\rho_{t+\epsilon}, t + \epsilon).$$

We can rearrange the inequality above and divide by ϵ to find

$$0 \geq \frac{1}{\epsilon} \int_t^{t+\epsilon} R(\rho_s, w) ds + \frac{V(\rho_{t+\epsilon}, t + \epsilon) - V(p, t)}{\epsilon}.$$

Taking $\epsilon \rightarrow 0$ and noticing $\rho_t = p$, we have

$$0 \geq R(p, w) + \partial_t V(p, t) + \left\langle \frac{\delta}{\delta p} V(p, t), \partial_t \rho_t \right\rangle.$$

Realizing $\partial_t \rho_t = -\nabla \cdot (w \rho_t) = -\nabla \cdot (w p)$ and using integration by parts, we have

$$0 \geq R(p, w) + \partial_t V(p, t) + \left\langle w \cdot \nabla \frac{\delta}{\delta p} V(p, t), p \right\rangle.$$

As we chose w arbitrarily, we can conclude

$$0 \geq \partial_t V(p, t) + \max_{w \in U} \left\{ \left\langle w \cdot \nabla \frac{\delta}{\delta p} V(p, t), p \right\rangle + R(p, w) \right\}. \quad (42)$$

Now we show the inequality in (42) is actually an equality. To this end, we consider any $(t, p) \in [0, T] \times P$, and let $u^* : [t, T] \times \Omega \rightarrow \mathbb{R}$ and $\rho^* : [t, T] \times \Omega \rightarrow \mathbb{R}$ be the optimal solution to the control problem defined by the value functional at $V(p, t)$ in (39). Then for any $\epsilon > 0$ we know by the optimality of ρ^* and $\rho_t^* = p$, there is

$$V(\rho_t^*, t) = \int_t^{t+\epsilon} R(\rho_s^*, u_s^*) ds + V(\rho_{t+\epsilon}^*, t + \epsilon).$$

We follow the same steps as before by dividing by ϵ , taking a limit $\epsilon \rightarrow 0$, and using integration by parts to find

$$0 = \partial_t V(\rho_t^*, t) + \left\langle u_t^* \cdot \nabla \frac{\delta}{\delta p} V(\rho_t^*, t), \rho_t^* \right\rangle + R(\rho_t^*, u_t^*). \quad (43)$$

Combining both (42) and (43), $\rho_t^* = p$, and $u_t^* \in U$, we conclude the maximum can be attained and the equality in (42) holds. This completes the proof. \square

Example 3.13. We continue with Example 3.10 with the running reward (27), terminal reward (28), and arbitrary initial value $\rho_0 = p > 0$.

Recall from (41) that the HJB equation is

$$\partial_t V(p, t) + \max_{w \in U} \left\{ \left\langle p, w \cdot \nabla \frac{\delta}{\delta p} V(p, t) \right\rangle - \frac{1}{2} \int_{\Omega} |w|^2 p dx \right\} = 0. \quad (44)$$

Inspired by the square completion in (33) and the optimal solution (38), we attempt $w = \frac{x}{t-T-1}$ as the maximizer in (44). Completing the square, we obtain $\nabla \frac{\delta}{\delta p} V(p, t) = w$, from which we deduce that

$$V(p, t) = \frac{1}{2(t-T-1)} \int_{\Omega} |x|^2 p(x) dx. \quad (45)$$

We can verify that $V(p, t)$ in (45) indeed satisfies the HJB equation (44) with the maximum attained at $w = \frac{x}{t-T-1}$ for all t . Moreover, the terminal value of $V(p, t)$ is

$$V(p, T) = -\frac{1}{2} \int_{\Omega} |x|^2 p(x) dx = G(p). \quad (46)$$

Notice that (45) also suggests the optimal control to be

$$u_t(x) = \nabla \frac{\delta}{\delta \rho_t} V(\rho_t, t) = \frac{x}{t-T-1}, \quad (47)$$

which agrees with (38).

3.3 Variations of Initial Perturbation

In this subsection, we consider the Fréchet derivative of $G(\rho_T)$ with respect to the initial value p , where $\rho : \Omega \times [0, T] \rightarrow \mathbb{R}$ solves the continuity equation (2) with initial value $\rho_0 = p$. The result demonstrates an important property of the adjoint function ϕ .

Suppose the initial states $\{x_i \in \Omega : i = 1, \dots, N\}$ of agents are perturbed, changing the initial probability p to

$$p^\epsilon := p + \epsilon h + o(\epsilon) \in P, \quad (48)$$

with some $h, o(\epsilon) : \Omega \rightarrow \mathbb{R}$ satisfying

$$\int_{\Omega} h(x) dx = 0, \quad \int_{\Omega} o(\epsilon) dx = 0. \quad (49)$$

Note that (49) is necessary for $p^\epsilon \in P$. Let ρ^ϵ solve the initial value problem:

$$\begin{cases} \partial_t \rho_i^\epsilon + \nabla \cdot (\rho_i^\epsilon u) = 0, & \forall t \in [0, T], \\ \rho_0^\epsilon = p^\epsilon. \end{cases} \quad (50)$$

We are interested in the difference between ρ_i^ϵ from (50) and ρ_t from (7b)–(7c), which use the same control vector field $u \in U_T$ but different initial values p^ϵ and p , respectively.

Lemma 3.14. *Let ρ_t^ϵ and ρ_t solve (50) with initials p^ϵ and p , respectively. Then*

$$\lim_{\epsilon \rightarrow 0} \sup_{0 \leq t \leq T} \frac{1}{\epsilon} \|\rho_t^\epsilon - \rho_t - \epsilon s_t\|_2 = 0, \quad (51)$$

where s_t solves the initial value problem:

$$\begin{cases} \partial_t s_t + \nabla \cdot (s_t u_t) = 0, & \forall t \in [0, T], \\ s_0 = h. \end{cases} \quad (52)$$

Proof. Define $\delta(t) := \frac{1}{2} \|\rho_t^\epsilon - \rho_t - \epsilon s_t\|_2^2$. Mimicking (19) with σ_t replaced by s_t , we obtain $\delta(t) \leq \delta(0)e^{dM_U T}$ for all $t \in [0, T]$. Since $\delta(0) = \frac{1}{2} \|p^\epsilon - p\|_2^2 = o(\epsilon^2)$, we know

$$\lim_{\epsilon \rightarrow 0} \sup_{0 \leq t \leq T} \frac{(2\delta(t))^{1/2}}{\epsilon} \leq \lim_{\epsilon \rightarrow 0} \frac{(2\delta(0))^{1/2}}{\epsilon} e^{dM_U T/2} = 0,$$

which justifies (51). □

Proposition 3.15. *For any $T > 0$, $u \in U_T$, initial value $p \in P$, let ρ_t be solution to the initial value problem*

$$\begin{cases} \partial_t \rho_t + \nabla \cdot (\rho_t u_t) = 0, & \forall t \in [0, T], \\ \rho_0 = p. \end{cases} \quad (53)$$

Then for any functional $G : P \rightarrow \mathbb{R}$ Fréchet differentiable in P , there is

$$\frac{\delta}{\delta p} G(\rho_T) = \phi_0, \quad (54)$$

where $p = \rho_0$ is the initial value of ρ , and ϕ solves the terminal value problem:

$$\begin{cases} \partial_t \phi_t + u_t \cdot \nabla \phi_t = 0, & \forall t \in [0, T], \\ \phi_T = \frac{\delta}{\delta \rho_T} G(\rho_T). \end{cases} \quad (55)$$

Proof. For any h with (49), let p^ϵ be the initial value defined in (48) and ρ^ϵ solve the initial value problem (50), we know by Lemma 3.14 that

$$G(\rho_T^\epsilon) = G(\rho_T + \epsilon s_T + o(\epsilon)), \quad (56)$$

where s_t is the solution to (52). Therefore

$$\frac{d}{d\epsilon} G(\rho_T^\epsilon) \Big|_{\epsilon=0} = \left\langle \frac{\delta}{\delta \rho_T} G(\rho_T), s_T \right\rangle = \langle \phi_T, s_T \rangle, \quad (57)$$

where the second equality is due to the terminal condition of ϕ_t in (55).

On the other hand, notice that

$$\begin{aligned} \frac{d}{dt} \langle \phi_t, s_t \rangle &= \langle \partial_t \phi_t, s_t \rangle + \langle \phi_t, \partial_t s_t \rangle \\ &= -\langle u_t \cdot \nabla \phi_t, s_t \rangle - \langle \phi_t, \nabla \cdot (s_t u_t) \rangle \\ &= 0, \end{aligned}$$

where the second equality is due to the PDE of ϕ in (55) and the PDE of s in (52); and the third equality is due to integration by parts and $(u_t \cdot n)|_{\partial\Omega} = 0$ on $\partial\Omega$. Therefore, $\langle \phi_t, s_t \rangle$ is constant in t and hence

$$\langle \phi_T, s_T \rangle = \langle \phi_0, s_0 \rangle = \langle \phi_0, h \rangle. \quad (58)$$

Combining (57) and (58), and noticing that $\frac{\delta}{\delta p} G(\rho_T) = \frac{d}{d\epsilon} G(\rho_T^\epsilon)|_{\epsilon=0}$, we obtain

$$\left\langle \frac{\delta}{\delta p} G(\rho_T), h \right\rangle = \langle \phi_0, h \rangle. \quad (59)$$

Since h is arbitrary, we know (54) holds. \square

Example 3.16. Let $T > 0$ and $p \in P$ be given arbitrarily and $\Omega = \mathbb{R}^d$. Define $u \in U_T$ by

$$u_t(x) = \frac{x}{2(t-T-1)} \quad (60)$$

for all $x \in \Omega$ and $t \in [0, T]$. Let ρ be the solution to (53) with the vector field u in (60) and initial value p . Define a functional $G : P \rightarrow \mathbb{R}$ such that

$$G(q) = -\frac{1}{2} \int_{\Omega} |x|^2 q(x) dx, \quad \forall q \in P. \quad (61)$$

Notice that $\frac{\delta}{\delta q} G(q) = -\frac{1}{2}|x|^2$ for all q .

We can verify that

$$\phi_t(x) = \frac{|x|^2}{2(t-T-1)} \quad (62)$$

is the solution to the terminal value problem (55) with u in (60) and terminal value $\phi_T = \frac{\delta}{\delta \rho_T} G(\rho_T) = -\frac{1}{2}|x|^2$.

Now, from Proposition 3.15, we claim that

$$\frac{\delta}{\delta p} G(\rho_T) = \phi_0 = -\frac{|x|^2}{2(T+1)}. \quad (63)$$

To justify the claim (63), we first notice that

$$\rho_t(x) = \left(\frac{T+1}{T+1-t} \right)^{d/2} p \left(\left(\frac{T+1}{T+1-t} \right)^{1/2} x \right)$$

is the solution to the initial value problem (53) with the vector field u in (60) and the given initial value p . Therefore

$$\rho_T(x) = (T+1)^{d/2} p(\sqrt{T+1}x).$$

Hence we obtain

$$\begin{aligned} G(\rho_T) &= -\frac{1}{2} \int_{\Omega} |x|^2 \rho_T(x) dx \\ &= -\frac{1}{2} \int_{\Omega} |x|^2 (T+1)^{d/2} p(\sqrt{T+1}x) dx \\ &= -\frac{1}{2(T+1)} \int_{\Omega} |y|^2 p(y) dy, \end{aligned}$$

where the last equality is due to the change of variables $y = \sqrt{T+1}x$. Therefore $\frac{\delta}{\delta p} G(\rho_T) = -\frac{|x|^2}{2(T+1)}$, which justifies (63).

4 Algorithmic Development

In this section, we develop a numerical algorithm in light of the maximum principle (Theorem 3.9) to solve the probability control problem (7). We provide a general description of this algorithm in Section 4.1 and some implementation details in Section 4.3.

4.1 Description of the Proposed Algorithm

The development of our algorithm was inspired by [5, 34], which are designed for classical optimal control problems. The idea is alternately updating (ρ, u) and ϕ . Namely, we begin with an initial guess u^0 , and find its corresponding ρ^0 . Let $k = 1, 2, \dots$ be the iteration number. In the k th iteration, we compute ϕ^k that satisfies the adjoint PDE (11) and terminal condition using (ρ^{k-1}, u^{k-1}) obtained in the previous iteration; compute (ρ^k, u^k) based on the maximum principle and the continuity equation using ϕ^k ; and then move on to the next iteration. We provide more details about this alternating update scheme in the Algorithm Iterations (Section 4.1.2) below.

In our experiments, we are interested in solving optimal probability control problem in high dimensions, e.g., $d \geq 10$. To this end, we parameterize $u : \mathbb{R}^d \times [0, T] \rightarrow \mathbb{R}^d$ and $\phi : \mathbb{R}^d \times [0, T] \rightarrow \mathbb{R}$ using reduced-order models. More specifically, we parameterize them as deep neural networks (DNNs). DNNs are effective function approximators by using finite amounts of network parameters. With DNN parameterizations, our algorithm does not require any spatial discretization as in traditional numerical PDE solvers, such as finite difference and finite element methods, which suffer the curse of dimensionality.

Since we use DNNs to parameterize u and ϕ , we need to update their network parameters in our numerical algorithm. For notation simplicity, we will also use u to denote its network parameters hereafter. For example, by solving for u^k in the k th iteration of our algorithm, we mean finding the optimal network parameters of u^k . The same for ϕ^k .

In our experiments, we artificially simulate a swarm of N agents, denoted by $\{x_i(t) \in \Omega : i = 1, \dots, N\}$, to represent the probability density function ρ_t . In other words, $\{x_i(t)\}$ are N samples following the probability ρ_t . Then the continuity equation (2) can be equivalently written as N trajectories solving the ODEs (1) with initials $x_i(0) \sim p$ with the current guess u . Our algorithm will track these ODEs jointly with u by the Neural ODE method [12].

Our algorithm is summarized in Algorithm 1. Next, we provide a description of the initialization, the iterations, and the termination criterion of this algorithm.

4.1.1 Initialization

We first determine the DNN architectures of ϕ and u . By network architecture, we meant the general structure, such as type, depth, width, and activation functions, of the network. The choice of such architecture is generally flexible. As $u : \mathbb{R}^d \times [0, T] \rightarrow \mathbb{R}^d$, we can parameterize it as a small neural network with input (t, x) , which is of dimension $d + 1$, and output $u(t, x)$, which is of dimension d . The same for ϕ but the output dimension is 1. To ensure u is Lipschitz continuous, we use smooth and globally Lipschitz activation functions, and restrict the parameter values within a bounded set.

We can initialize u^0 randomly using common network initialization method. This can be improved if one can provide an initial guess vector field with explicit formula that is close to the true $u(t, x)$, and train u^0 to approximate this initial guess field as the actual initial. Then we generate

Algorithm 1 Numerical method for solving (7)

Input: Initial guess u^0 , sample size N , $k = 1$, max iteration number K , and tolerance $\epsilon_{\text{tol}} > 0$.

- 1: Generate i.i.d. samples $x_i(0) \sim p$ for $i = 1, \dots, N$.
- 2: Solve the ODEs $x'_i(t) = u_t^0(x_i(t))$ to represent ρ_t^0 .
- 3: **while** $k \leq K$ **do**
- 4: Set ϕ^k to the minimizer of (64).
- 5: Set (ρ^k, u^k) to the minimizer (65), where ρ_t^k is represented as $\{x_i^k(t) : i = 1, \dots, N\}$.
- 6: **if** $\int_0^T \|u_t^{k+1} - u_t^k\|_2^2 dt < \epsilon_{\text{tol}}$ **then**
- 7: Break.
- 8: **else**
- 9: $k \leftarrow k + 1$.
- 10: **end if**
- 11: **end while**

Output: Optimal control vector field u^k .

samples $\{x_i(t) : i = 1, \dots, N, 0 \leq t \leq T\}$ by solving the ODEs (1) as described above using u^0 , and these samples represent ρ^0 . Now we have an initial (ρ^0, u^0) . We also select a maximum iteration number $K \in \mathbb{N}$ and a tolerance $\epsilon_{\text{tol}} > 0$ for termination criterion.

4.1.2 Algorithm Iterations

Let $k = 1, \dots, K$ be the iteration number. In the k th iteration, we have (ρ^{k-1}, u^{k-1}) from the previous iteration (or initial guess), and compute ϕ^k and (ρ^k, u^k) in order as below.

To compute ϕ^k , we need to solve the adjoint PDE (11) and the corresponding terminal condition using (ρ^{k-1}, u^{k-1}) . To this end, we apply the method of physics-informed neural network (PINN) [32] by formulating the loss function of ϕ^k as the squared error in the adjoint PDE subject to the terminal condition. Namely, we set ϕ^k to be the minimizer of the following loss function

$$\int_0^T \int_{\Omega} \left| \partial_t \phi_t + u_t^k \cdot \nabla \phi_t + \frac{\delta}{\delta \rho_t^{k-1}} R(\rho_t^{k-1}, u_t^{k-1}) \right|^2 dx dt \quad (64)$$

subject to $\phi_T^k = \frac{\delta}{\delta \rho_T^{k-1}} G(\rho_T^{k-1})$. The PINN method approximates the integral like (64) by Monte Carlo integration. See the implementation details of this approximation for (64) in Section 4.3 below. The constraint can be relaxed by replacing it with a penalty term $\mu \|\phi_T - \frac{\delta}{\delta \rho_T^{k-1}} G(\rho_T^{k-1})\|_2^2$, where $\mu > 0$ is the penalty weight parameter, added to the loss function (64). Alternatively, we can use a simple trick of network architecture set up such that this constraint is automatically satisfied, as we show in Section 5 below.

Besides PINN, there are other methods that can be adopted to solve (64). In particular, the adjoint PDE (11) is a first-order linear evolution PDE backward in time with a terminal value, it can be solved by converting the problem to solving an ODE of the network parameters backward in time [15]. In the present work, we use PINN for simplicity.

Once ϕ^k is obtained, we invoke the maximum principle (21) and set (ρ^k, u^k) as the minimizer of the following loss function with proximal point regularization:

$$-\int_0^T H(\rho_t, \phi_t^k, u_t) dt + \frac{1}{2\varepsilon_k} \int_0^T \|u_t - u_t^k\|_2^2 dt, \quad (65)$$

subject to $\partial_t \rho_t + \nabla \cdot (\rho_t u_t) = 0$ and $\rho_0 = p$. Here $\varepsilon_k > 0$ is the step size. We use the Neural ODE method [12] to find the gradient of the loss function with respect to the parameters of u . To use this method, we can artificially simulate N agents $\{x_i(t) : i = 1, \dots, N, 0 \leq t \leq T\}$ to represent ρ^k and finds the optimal u jointly. Note that this ensures that the continuity equation and initial condition of ρ^k are automatically satisfied.

4.1.3 Termination Criterion

We terminate the algorithm if k reaches the maximum iteration number K or $\int_0^T \|u_t^{k+1} - u_t^k\|_2^2 dt < \epsilon_{\text{tol}}$ as set in the initialization step.

There are some additional problem-specific details about solving the minimization subproblems in practical implementation. We will provide them in Section 4.3. We now show that Algorithm 1 converges under certain conditions.

4.2 Convergence Analysis of the Proposed Algorithm

We consider the convergence of Algorithm 1 in solving the density control problem (7) in this subsection. Specially, we will prove several convergence properties of the sequence $\{u^k\}$ generated by Algorithm 1 from any initial u^0 . The convergence proofs require several additional assumptions, which we will highlight in this subsection.

Assumption 4.1. *There exists $M_\rho > 0$ such that, for all $u \in U_T$, the corresponding density ρ started from initial p and controlled by u satisfies $\|\nabla \rho_t\|_\infty \leq M_\rho$ for all $t \in [0, T]$.*

Assumption 4.1 is valid if $\|\nabla p\|_\infty = \sup_{x \in \Omega} |\nabla p(x)|$ is finite and we also impose a uniform upper bound on all u in U_T , with a fixed finite T in consideration. In real-world applications, the agents (such as robots) representing ρ_t along time t maintain certain distances from each other to prevent collisions, as considered in our experiments below. In this case, penalty on large $\nabla \rho_t$ is implicitly imposed and Assumption 4.1 holds.

Lemma 4.2. *Suppose Assumption 4.1 holds. Let $u, v \in U_T$ and $\rho, \pi \in P_T$, where ρ and π are independently driven by u and v , i.e., satisfy the continuity equations with time-dependent vector fields u and v , from two initial values $p \in P$ and $q \in P$, respectively. Define $E(h) := \frac{1}{2} \|\rho_h - \pi_h\|_2^2$ for all $h \geq 0$. Then*

$$\dot{E}(0) \leq \sqrt{2} M_\rho \sqrt{E(0)} \|u_0 - v_0\|_2 + dM_U E(0). \quad (66)$$

Proof. Let $x_h(z)$ be the push-forward of $z \in \Omega$ by u up to time h , i.e., $x_h(z)$ is the solution $x(t; z)$ of the initial value problem

$$\begin{cases} \frac{d}{dt} x(t; z) = u_t(x(t; z)), & \forall t \in [0, h] \\ x(0; z) = z, \end{cases}$$

at time $t = h$, namely $x_h(z) = x(h; z)$. Let $y_h(z)$ be defined in the same way but with v instead.

For all $h > 0$ sufficiently small, we know there exist $\tilde{u}, \tilde{v} : \Omega \times [0, h] \rightarrow \mathbb{R}^d$ with

$$\|\nabla \tilde{u}\|_\infty, \|\nabla \tilde{v}\|_\infty, \|\partial_h \tilde{u}\|_\infty, \|\partial_h \tilde{v}\|_\infty \leq M_{U,h}$$

on $\Omega \times [0, h]$ for some $M_{U,h} > 0$, such that the x_h and y_h can be represented (e.g., by Taylor expansion) as

$$x_h(z) = z + u_0(z)h + \tilde{u}_0(z, h)h^2, \quad (67a)$$

$$y_h(z) = z + v_0(z)h + \tilde{v}_0(z, h)h^2, \quad (67b)$$

and they are both bijective on Ω , and $\det(\nabla_z x_h(z)), \det(\nabla_z y_h(z)) > 0$ for all $z \in \Omega$. We used, for example, $u_t(\cdot)$ to represent $u(\cdot, t)$ for short in (67a) and (67b). In addition, notice that all of x_0, y_0, x_0^{-1} , and y_0^{-1} are the identity map. Since

$$\begin{aligned} E(h) &= \frac{1}{2} \int_\Omega |\rho_h(x_h(z)) - \pi_h(x_h(z))|^2 dx_h(z) \\ &= \frac{1}{2} \int_\Omega |\rho_0(z) - \pi_h(y_h(y_h^{-1}(x_h(z))))|^2 \det(\nabla_z x_h(z)) dz \\ &= \frac{1}{2} \int_\Omega |\rho_0(z) - \pi_0(y_h^{-1}(x_h(z)))|^2 \det(\nabla_z x_h(z)) dz, \end{aligned} \quad (68)$$

where the second and third equalities are due to the fact $\rho_h(x_h(w)) = \rho_0(w)$ and $\pi_h(y_h(w)) = \pi_0(w)$ for any $w \in \Omega$ since x_h and y_h , as well as x_h^{-1} and y_h^{-1} , are bijective. Thus, we have

$$\begin{aligned} \dot{E}(h) &= - \int_\Omega (\rho_0(z) - \pi_0(y_h^{-1}(x_h(z)))) \nabla \pi_0(y_h^{-1}(x_h(z))) \cdot J_1(z, h) \det(\nabla_z x_h(z)) dz \\ &\quad + \frac{1}{2} \int_\Omega |\rho_0(z) - \pi_0(y_h^{-1}(x_h(z)))|^2 J_2(z, h) dz \end{aligned} \quad (69)$$

where J_1 and J_2 are defined as

$$J_1(z, h) := \frac{d}{dh}(y_h^{-1}(x_h(z))) \in \mathbb{R}^d, \quad (70a)$$

$$J_2(z, h) := \frac{d}{dh}(\det(x_h(z))) \in \mathbb{R}. \quad (70b)$$

Note that we have

$$\frac{d}{dh}x_h(z) = \frac{d}{dh}(y_h(y_h^{-1}(x_h(z)))) = \partial_h y_h(y_h^{-1}(x_h(z))) + \nabla y_h(y_h^{-1}(x_h(z)))J_1(z, h). \quad (71)$$

By taking $h = 0$, we see the left-hand side of (71) is

$$\left. \frac{d}{dh}x_h(z) \right|_{h=0} = u_0(z) \quad (72)$$

and the right-hand side of (71) is

$$\begin{aligned} &\partial_h y_h(y_h^{-1}(x_h(z)))|_{h=0} + \nabla y_h(y_h^{-1}(x_h(z)))|_{h=0} J_1(z, h)|_{h=0} \\ &= [v_0(y_h^{-1}(x_h(z))) + 2h\tilde{v}_0(y_h^{-1}(x_h(z)), h) + \partial_h \tilde{v}_0(y_h^{-1}(x_h(z)), h)h^2]|_{h=0} \\ &\quad + [I_d + \nabla v_0(y_h^{-1}(x_h(z)))h + \nabla \tilde{v}_0(y_h^{-1}(x_h(z)), h)h^2]|_{h=0} J_1(z, h)|_{h=0} \\ &= v_0(z) + J_1(z, 0). \end{aligned} \quad (73)$$

where I_d is the $d \times d$ identity matrix. Plugging (72) and (73) into (71), we obtain

$$J_1(z, 0) = u_0(z) - v_0(z). \quad (74)$$

Furthermore, we know by the Jacobi formula that for any matrix-valued function $A : \mathbb{R} \rightarrow \mathbb{R}^{d \times d}$ which is invertible at h , there is

$$\frac{d}{dh} \det(A(h)) = \det(A(h)) \operatorname{tr} \left(A(h)^{-1} \frac{d}{dh} A(h) \right).$$

Therefore, for any $z \in \Omega$, there are

$$\nabla_z x_h(z)|_{h=0} = (I_d + \nabla u_0(z)h + \nabla \tilde{u}_0(z, h)h^2)|_{h=0} = I_d,$$

and

$$\frac{d}{dh} \nabla_z x_h(z)|_{h=0} = \frac{d}{dh} (I_d + \nabla u_0(z)h + \nabla \tilde{u}_0(z, h)h^2)|_{h=0} = \nabla u_0(z),$$

and hence

$$J_2(z, 0) = \det(\nabla_z x_h(z)|_{h=0}) \operatorname{tr} \left(\nabla_z x_h(z)^{-1}|_{h=0} \frac{d}{dh} \nabla_z x_h(z)|_{h=0} \right) = \operatorname{tr}(\nabla u_0(z)) = \nabla \cdot u_0(z). \quad (75)$$

Therefore, by taking $h = 0$ and (74) and (75), we obtain from (69) that

$$\begin{aligned} \dot{E}(0) &= - \int_{\Omega} (\rho_0(z) - \pi_0(z)) \nabla \pi_0(z) \cdot (u_0(z) - v_0(z)) dz + \frac{1}{2} \int_{\Omega} |\rho_0(z) - \pi_0(z)|^2 (\nabla \cdot u_0(z)) dz \\ &\leq M_{\rho} \|\rho_0 - \pi_0\|_2 \|u_0 - v_0\|_2 + \frac{dM_U}{2} \|\rho_0 - \pi_0\|_2^2, \end{aligned}$$

where we used Assumption 4.1 to obtain $\|\nabla \pi_0\|_{\infty} \leq M_{\rho}$ in the inequality. Therefore, (66) is justified. \square

Proposition 4.3. *Consider the same setting as in Lemma 4.2 but with an identical initial value $\rho_0 = \pi_0$. Then for any $t \in [0, T]$, there is*

$$\frac{d}{dt} \left(\frac{1}{2} \|\rho_t - \pi_t\|_2^2 \right) \leq \sqrt{2} M_{\rho} \|u_t - v_t\|_2 \left(\frac{1}{2} \|\rho_t - \pi_t\|_2^2 \right)^{1/2} + \frac{dM_U}{2} \|\rho_t - \pi_t\|_2^2. \quad (76)$$

Furthermore, there is

$$\frac{1}{2} \|\rho_t - \pi_t\|_2^2 \leq M_{\rho}^2 t e^{dM_U t} \int_0^t \frac{1}{2} \|u_s - v_s\|_2^2 ds. \quad (77)$$

Proof. The bound (76) is directly implied by Lemma 4.2 with 0 replaced by any arbitrary $t \in [0, T]$. To show (77), we define $\delta(t) := \frac{1}{2} \|\rho_t - \pi_t\|_2^2$. Then by (76) we have

$$\dot{\delta}(t) = dM_U \delta(t) + \sqrt{2} M_{\rho} \|u_t - v_t\|_2 \sqrt{\delta(t)}. \quad (78)$$

Dividing both sides by $2\sqrt{\delta(t)}$, we obtain

$$\frac{\dot{\delta}(t)}{2\sqrt{\delta(t)}} = \frac{d}{dt} \sqrt{\delta(t)} = \frac{dM_U}{2} \sqrt{\delta(t)} + \frac{M_{\rho}}{\sqrt{2}} \|u_t - v_t\|_2.$$

By the Grönwall inequality, we have

$$\sqrt{\delta(t)} \leq \left(\sqrt{\delta(0)} + \frac{M_\rho}{\sqrt{2}} \int_0^t \|u_s - v_s\|_2 e^{-dM_U s/2} ds \right) e^{dM_U t/2} \leq \frac{1}{\sqrt{2}} M_\rho e^{dM_U t/2} \int_0^t \|u_s - v_s\|_2 ds,$$

where $\delta(0) = 0$ since $\rho_0 = \pi_0$. Therefore, we obtain

$$\frac{1}{2} \|\rho_t - \pi_t\|_2^2 = \delta(t) \leq \frac{1}{2} M_\rho^2 e^{dM_U t} \left(\int_0^t \|u_s - v_s\|_2 ds \right)^2 \leq \frac{1}{2} M_\rho^2 t e^{dM_U t} \int_0^t \|u_s - v_s\|_2^2 ds$$

where the last inequality is due to the Cauchy–Schwarz inequality. This justifies (77). \square

Assumption 4.4. *We make the following assumptions:*

- (i) $\frac{\delta}{\delta\rho}H$ and $\frac{\delta}{\delta\rho}G$ are L_ρ - and L_G -Lipshitz in ρ , respectively, and $\frac{\delta}{\delta u}H$ is L_u -Lipshitz in u , for some $L_\rho, L_G, L_u > 0$.
- (ii) H is concave in u .

Theorem 4.5. *Suppose Assumptions 4.1 and 4.4 hold. Let $c > 0$ be arbitrary. Denote*

$$\varepsilon_{\max} := \frac{2}{L_u + (L_\rho T + L_G) M_\rho^2 dM_U + c} \quad (79)$$

and choose $\varepsilon_{\min} \in (0, \varepsilon_{\max})$ arbitrarily. Let $\{(\rho^k, \phi^k, u^k) : k \in \mathbb{N}\}$ be a sequence generated by Algorithm 1 with ε_k chosen from $[\varepsilon_{\min}, \varepsilon_{\max}]$ for every k and any initial guess $u^0 \in U$. Then

- (i) $I[u^k]$ is non-decreasing.
- (ii) If in addition Ω is bounded and $\{u^k\}$ is uniformly bounded, then $\{u^k\}$ has at least one uniformly convergent subsequence with some limit $\hat{u} \in U_T$. Moreover, $I[u^k] \rightarrow I[\hat{u}]$.

Proof. (i) For notation simplicity, we denote

$$\alpha^k := u^{k+1} - u^k, \quad \beta^k := \rho^{k+1} - \rho^k,$$

and

$$H_t^k := H(\rho_t^k, \phi_t^k, u_t^k) = \langle \rho_t^k, u_t^k \cdot \nabla \phi_t^k \rangle + R(\rho_t^k, u_t^k).$$

Recall the definition of total reward functional I in (7) and the Hamiltonian functional H in (12), we have

$$I[u^k] = \int_0^T \left(H_t^k - \langle \rho_t^k, u_t^k \cdot \nabla \phi_t^k \rangle \right) dt + G(\rho_T^k)$$

and

$$I[u^{k+1}] = \int_0^T \left(H(\rho_t^{k+1}, \phi_t^k, u_t^{k+1}) - \langle \rho_t^{k+1}, u_t^{k+1} \cdot \nabla \phi_t^k \rangle \right) dt + G(\rho_T^{k+1}).$$

Therefore,

$$\begin{aligned} I[u^k] - I[u^{k+1}] &= \int_0^T \left[H_t^k - H(\rho_t^{k+1}, \phi_t^k, u_t^{k+1}) + \langle \rho_t^{k+1}, u_t^{k+1} \cdot \nabla \phi_t^k \rangle - \langle \rho_t^k, u_t^k \cdot \nabla \phi_t^k \rangle \right] dt \\ &\quad - G(\rho_T^{k+1}) + G(\rho_T^k) \\ &= \int_0^T \left[H(\rho_t^k, \phi_t^k, u_t^k) - H_t^k + \langle \partial_t \beta_t^k, \phi_t^k \rangle \right] dt - G(\rho_T^{k+1}) + G(\rho_T^k), \end{aligned} \quad (80)$$

where we used integration by parts, the continuity equations of ρ^k and ρ^{k+1} with u^k and u^{k+1} respectively, and the definition of β^k to obtain the second equality. With Assumption 4.4 (i) on the Lipschitz continuity of $\frac{\delta H}{\delta u}$ and $\frac{\delta H}{\delta \rho}$ (and $-\frac{\delta H}{\delta \rho}$ as well), we have

$$H(\rho_t^{k+1}, \phi_t^k, u_t^k) \leq H(\rho_t^{k+1}, \phi_t^k, u_t^{k+1}) - \left\langle \frac{\delta}{\delta u_t^{k+1}} H(\rho_t^{k+1}, \phi_t^k, u_t^{k+1}), \alpha_t^k \right\rangle + \frac{L_u}{2} \|\alpha_t^k\|_2^2 \quad (81)$$

and

$$-H(\rho_t^{k+1}, \phi_t^k, u_t^k) \leq -H_t^k - \left\langle \frac{\delta}{\delta \rho_t^k} H_t^k, \beta_t^k \right\rangle + \frac{L_\rho}{2} \|\beta_t^k\|_2^2. \quad (82)$$

Combining (81) and (82) yields

$$H_t^k - H(\rho_t^{k+1}, \phi_t^k, u_t^{k+1}) \leq -\left\langle \frac{\delta}{\delta u_t^{k+1}} H(\rho_t^{k+1}, \phi_t^k, u_t^{k+1}), \alpha_t^k \right\rangle - \left\langle \frac{\delta}{\delta \rho_t^k} H_t^k, \beta_t^k \right\rangle + \frac{L_u}{2} \|\alpha_t^k\|_2^2 + \frac{L_\rho}{2} \|\beta_t^k\|_2^2. \quad (83)$$

With Assumption 4.4 (ii), the convexity of U_T and the optimality condition of u^{k+1} in the update step of (ρ^{k+1}, u^{k+1}) in Algorithm 1, we have

$$\left\langle -\frac{\delta}{\delta u_t^{k+1}} H(\rho_t^{k+1}, \phi_t^k, u_t^{k+1}) + \frac{1}{\varepsilon_k} \alpha_t^k, \alpha_t^k \right\rangle \leq 0. \quad (84)$$

Plugging (83), (84), and $\partial_t \phi_t^k = -\frac{\delta}{\delta \rho_t^k} H_t^k$ (Proposition 3.5) into (80), we obtain

$$\begin{aligned} I[u^k] - I[u^{k+1}] &\leq \int_0^T \left(-\frac{1}{\varepsilon_k} \|\alpha_t^k\|_2^2 + \frac{L_u}{2} \|\alpha_t^k\|_2^2 + \frac{L_\rho}{2} \|\beta_t^k\|_2^2 \right) dt \\ &\quad + \int_0^T \left(\langle \partial_t \phi_t^k, \beta_t^k \rangle + \langle \phi_t^k, \partial_t \beta_t^k \rangle \right) dt - G(\rho_T^{k+1}) + G(\rho_T^k). \end{aligned} \quad (85)$$

Since $\rho_0^{k+1} = \rho_0^k = p$ which implies $\beta_0^k = 0$, we have

$$\int_0^T \left(\langle \partial_t \phi_t^k, \beta_t^k \rangle + \langle \phi_t^k, \partial_t \beta_t^k \rangle \right) dt = \langle \beta_T^k, \phi_T^k \rangle \Big|_0^T = \langle \beta_T^k, \phi_T^k \rangle = \left\langle \rho_T^{k+1} - \rho_T^k, \frac{\delta}{\delta \rho_T^k} G(\rho_T^k) \right\rangle. \quad (86)$$

With Assumption 4.4 (i) on the Lipschitz condition of $\frac{\delta}{\delta \rho} G$ (and $-\frac{\delta}{\delta \rho} G$ as well), we have

$$-G(\rho_T^{k+1}) + G(\rho_T^k) + \left\langle \frac{\delta}{\delta \rho_T^k} G(\rho_T^k), \rho_T^{k+1} - \rho_T^k \right\rangle \leq \frac{L_G}{2} \|\rho_T^{k+1} - \rho_T^k\|_2^2 = \frac{L_G}{2} \|\beta_T^k\|_2^2. \quad (87)$$

Applying (85), (86), and (87), we obtain

$$I[u^k] - I[u^{k+1}] \leq \int_0^T \left(-\frac{1}{\varepsilon_k} \|\alpha_t^k\|_2^2 + \frac{L_u}{2} \|\alpha_t^k\|_2^2 + \frac{L_\rho}{2} \|\beta_t^k\|_2^2 \right) dt + \frac{L_G}{2} \|\beta_T^k\|_2^2. \quad (88)$$

Due to the estimate (77) in Proposition 4.3, we have

$$\frac{1}{2} \|\beta_t^k\|_2^2 \leq M_\rho^2 dM_U t \int_0^t \frac{1}{2} \|\alpha_s^k\|_2^2 ds \leq M_\rho^2 dM_U T \int_0^T \frac{1}{2} \|\alpha_t^k\|_2^2 dt$$

for any $t \in [0, T]$, which further implies that

$$\frac{L_\rho}{2} \int_0^T \|\beta_t^k\|_2^2 dt \leq L_\rho M_\rho^2 dM_U T^2 \int_0^T \frac{1}{2} \|\alpha_t^k\|_2^2 dt, \quad (89)$$

$$\frac{L_G}{2} \|\beta_T^k\|_2^2 \leq L_G M_\rho^2 dM_U T \int_0^T \frac{1}{2} \|\alpha_t^k\|_2^2 dt. \quad (90)$$

Applying (89) and (90) into (88), we obtain

$$I[u^k] - I[u^{k+1}] \leq \left(-\frac{2}{\varepsilon_k} + L_u + (L_\rho T + L_G) M_\rho^2 dM_U \right) \int_0^T \frac{1}{2} \|\alpha_t^k\|_2^2 dt \quad (91)$$

Therefore, with $\varepsilon_k \in [\varepsilon_{\min}, \varepsilon_{\max}]$ for every k , we have $-\frac{2}{\varepsilon_k} + L_u + (L_\rho T + L_G) M_\rho^2 dM_U \leq -c < 0$ and thus from (91) there is

$$c \int_0^T \frac{1}{2} \|\alpha_t^k\|_2^2 dt \leq I[u^{k+1}] - I[u^k]. \quad (92)$$

This implies $I[u^k]$ is non-increasing.

(ii) By taking sum of (92) over $k = 0, \dots, K-1$ for any $K \in \mathbb{N}$, we obtain

$$c \sum_{k=0}^{K-1} \int_0^T \frac{1}{2} \|\alpha_t^k\|_2^2 dt \leq I[u^K] - I[u^0] \leq I^* - I[u^0] < \infty,$$

since $I[u^K] \leq I^* < \infty$ for all K . Letting $K \rightarrow \infty$, we know the series on the left-hand side converges, and thus

$$\|u^{k+1} - u^k\|_{L^2(\bar{\Omega}_T)}^2 = \int_0^T \|\alpha_t^k\|_2^2 dt \rightarrow 0.$$

This also implies that $\|u_t^{k+1} - u_t^k\|_{L^2(\bar{\Omega})} \rightarrow 0$ as $k \rightarrow \infty$ in $[0, T]$ almost everywhere.

Since $\Omega \in \mathbb{R}^d$ is bounded, we know $\bar{\Omega}_T := \bar{\Omega} \times [0, T]$ is compact in \mathbb{R}^{d+1} . Provided $\{u^k\} \subset U_T$ (hence u^k is M_U -Lipschitz continuous for all k) and $\|u^k\|_\infty$ are uniformly bounded, we know by the Arzelà–Ascoli theorem that there exists a subsequence $\{u^{k_j} : j \in \mathbb{N}\}$ of $\{u^k\}$ and $\hat{u} \in U_T$, such that $u^{k_j} \rightarrow \hat{u}$ uniformly. As $\|u^{k+1} - u^k\|_{L^2(\bar{\Omega}_T)} \rightarrow 0$, we know $u^{k_j-1} \rightarrow \hat{u}$ as $j \rightarrow \infty$ in $\bar{\Omega}_T$ in the L^2 sense.

Let $\hat{\rho}$ be the solution to (2) with vector field \hat{u} and initial value p . Notice that $\hat{\rho} \in P_T$ as $\hat{u} \in U_T$. By Proposition 4.3, more specifically, (77), we have for all $t \in [0, T]$ that

$$\|\rho_t^{k_j-1} - \hat{\rho}_t\|_2^2 \leq 2M_\rho^2 T e^{dM_U T} \|u^{k_j-1} - \hat{u}\|_{L^2(\bar{\Omega}_T)}^2 \rightarrow 0$$

as $j \rightarrow \infty$. Taking integral of t over $[0, T]$ on both sides above, we know $\rho^{k_j-1} \rightarrow \hat{\rho}$ as $j \rightarrow \infty$ in $\bar{\Omega}_T$ in the L^2 sense.

Let $\hat{\phi}$ be the adjoint function of $(\hat{\rho}, \hat{u})$ as in Definition 3.2. Notice that the adjoint PDE is a first-order linear PDE. Therefore ϕ^{k_j} , which is the adjoint of $(\rho^{k_j-1}, u^{k_j-1})$, converges to $\hat{\phi}$ as $j \rightarrow \infty$ in $\bar{\Omega}_T$ in the L^2 sense.

Next, we show that $(\hat{\rho}, \hat{\phi}, \hat{u})$ satisfies the Maximum Principle in Theorem 3.9. By the definitions of $\hat{\rho}$ and $\hat{\phi}$, we know they satisfy the Hamiltonian dynamics (13) with control vector field \hat{u} .

Furthermore, by the optimality condition of u^{k_j} , the convexity of U_T , and Assumption 4.4 (ii), we have for any $u \in U_T$ that

$$0 \leq \left\langle -\frac{\delta}{\delta u_t^{k_j}} H(\rho_t^{k_j}, \phi_t^{k_j}, u_t^{k_j}) + \frac{1}{\varepsilon_{k_j}} (u_t^{k_j} - u_t^{k_j-1}), u_t - u_t^{k_j} \right\rangle \quad (93)$$

for all $t \in [0, T]$. Taking $j \rightarrow \infty$, and noticing that $\varepsilon_{k_j} \geq \varepsilon_{\min} > 0$ and $\|u_t^{k_j} - u_t^{k_j-1}\|_{L^2(\Omega)} \rightarrow 0$ for all t , we obtain

$$0 \leq \left\langle -\frac{\delta}{\delta \hat{u}} H(\hat{\rho}_t, \hat{\phi}_t, \hat{u}_t), u_t - \hat{u}_t \right\rangle.$$

As H is concave in u , U_T is a convex set, and $u_t, \hat{u}_t \in U$, we see $H(\hat{\rho}_t, \hat{\phi}_t, \hat{u}_t) = \max_{u_t \in U} H(\hat{\rho}_t, \hat{\phi}_t, u_t)$.

Since $u^{k_j} \rightarrow \hat{u}$ uniformly, we have $I[u^{k_j}] \rightarrow I[\hat{u}]$. Combining with (i) and $\{u^{k_j}\}$ being a subsequence of $\{u^k\}$, we know $I[u^k] \rightarrow I[\hat{u}]$. \square

4.3 Implementation Details

In this subsection, we provide some details about our numerical implementations in minimizing (64) and (65).

For (64), we use the PINN method [32]. More specifically, we sample N points $\{(t_i, x_i) : i \in [N]\}$ uniformly from $[0, T] \times \Omega$, and approximate the (64) by

$$\frac{T|\Omega|}{N} \sum_{i=1}^N \left| \partial_t \phi_{t_i}(x_i) + u_{t_i}^k(x_i) \cdot \nabla \phi_{t_i}(x_i) + \frac{\delta}{\delta \rho_{t_i}^{k-1}} R(\rho_{t_i}^{k-1}, u_{t_i}^k)(x_i) \right|^2. \quad (94)$$

It is known that (64) is an unbiased estimation of the loss function (94), and the variance reduces at the rate of $O(N^{-1/2})$.

If Ω is unbounded, we can adopt the importance sampling method which samples x_i 's from a reference density p_{ref} supported on Ω and can be evaluated (e.g., p_{ref} is Gaussian if $\Omega = \mathbb{R}^d$) and divide the i th term of the summation in the loss function by $p_{\text{ref}}(x_i)$ in (94).

For (65), we recall the definition of H in (12) and approximate the loss function by

$$-\frac{T}{N_\Omega N_T} \sum_{j=1}^{N_T} \sum_{i=1}^{N_\Omega} u_{t_j}(x_i(t_j)) \cdot \nabla \phi_{t_j}^k(x_i(t_j)) - \frac{T|\Omega|}{N} \sum_{i=1}^N R(\rho_{\hat{t}_i}, u_{\hat{t}_i})(\hat{x}_i) + \frac{T|\Omega|}{2\varepsilon_k N} \sum_{i=1}^N |u_{\hat{t}_i}(\hat{x}_i) - u_{\hat{t}_i}^k(\hat{x}_i)|^2, \quad (95)$$

where $\{x_i(t_j) : i = 1, \dots, N_\Omega, j = 1, \dots, N_T\}$ are the states of artificially simulated agents at sampled time points in $[0, T]$ such that $x_i(t_j) \sim \rho_{t_j}$, and $\{(\hat{t}_i, \hat{x}_i) : i = 1, \dots, N\}$ are N points uniformly sampled from $[0, T] \times \Omega$. Then we apply the Neural ODE method to solve for (ρ^k, u^k) which minimizes (95) while satisfying the continuity equation and initial condition, where $\rho_{\hat{t}_j}^k$ is represented by the artificially simulated agents $\{x_i(t_j) : i = 1, \dots, N_\Omega\}$ for all t_j .

There are various treatments to handle the terms in the loss functions (94) and (95). For example, if $R(\rho_t, u_t) = -\frac{1}{2} \int_\Omega |u_t|^2 \rho_t dx$, then it can be approximated by the Monte Carlo integration

$$-\frac{1}{2} \frac{T}{N_\Omega N_T} \sum_{j=1}^{N_T} |u_{t_j}(x_i(t_j))|^2,$$

instead of the first term in the second line of (95). In the case where $R(\rho_t, u_t)$ contains a term

$$\int_{\Omega} \int_{\Omega} a(x, y) \rho_t(y) \rho_t(x) dy dx,$$

due to agent interaction specified by $a(x, y)$, we can simplify the computation of $R(\rho_t, u_t)$ and $\frac{\delta}{\delta \rho_t} R(\rho_t, u_t)$ by using an augmented variable $z := (x, y) \in \mathbb{R}^{2d}$ and setting its probability density as $\bar{\rho}(z) := \rho(x)\rho(y)$ and the control on z to $(u(x), u(y))$. This makes the approximation of $R(\rho_t, u_t)$ and $\frac{\delta}{\delta \rho_t} R(\rho_t, u_t)$ easier to implement in practice. We adopt these treatments throughout our experiments to simplify (94) and (95). We will release the code containing these details to the public upon the acceptance of this paper.

5 Experimental settings and results

We conduct several numerical experiments to demonstrate the performance of Algorithm 1 in solving the optimal probability control problem (7). In these experiments, we only consider the case where the terminal reward function is given by $G(q) = \int_{\Omega} g(x)q(x) dx$, and thus $\frac{\delta}{\delta q} G(q) = g$ for all $q \in P$. We will specify g in each experiment below.

In our numerical implementation, we parameterize u as a standard residual network (ResNet) with two hidden layers, each of width 100, and ReLU as the activation functions. We parameterize ϕ as

$$\phi_t(x) := \left(1 - \frac{t}{T}\right) \varphi(t, x) + \frac{t}{T} g(x), \quad (96)$$

where φ is also a ResNet with two hidden layers and width 100, and tanh as activation functions. The setting (96) ensures that the terminal condition $\phi_T = g$ is always satisfied, hence eliminating this constraint in implementation.

In each iteration of Algorithm 1, we update ϕ^k by applying the Adam optimizer [26] to minimize the empirical loss function (94) using a mini-batch of $N = 2,048$ newly drawn sample points for each iteration, with the default setting of $\beta_1 = 0.9$ and $\beta_2 = 0.999$ for 3,000 steps (except for $k = 1$ when we run 10,000 steps). We also adopt the Adam optimizer to update (ρ^k, u^k) jointly as in (95) with the same parameters for 20 steps, where in each step we apply the Neural ODE method to compute the gradient of the loss function with respect to the network parameters of u . For simplicity, we set the step size $\varepsilon_k = 0.25$ for all k . Experiments are conducted using PyTorch on a Windows 10 machine with one NVIDIA RTX GeForce 2080 Super GPU. All experiments in this section took a maximum of 10 minutes to complete the process outlined in Algorithm 1.

For demonstration purposes, we conduct numerical experiments on three synthetic test problems:

- Test 1 with agent interactions and problem domain Ω of dimension $d = 8$;
- Test 2 with a cylindrical obstacle and problem dimensions $d = 30$ and $d = 100$;
- Test 3 with agent interactions and a double-wedge obstacle in problem dimension $d = 30$.

Since there are no closed form solutions for these test problems, we cannot compute the numerical errors of our results. Instead, we provide some visual demonstrations of these results as shown in the figures below.

5.1 Test 1 with Agent Interactions

We consider an optimal probability control problem where the running reward functional contains a nonlinear agent interaction term. The problem domain is set to $\Omega = \mathbb{R}^d$ with $d = 8$, and the running reward functional is set to

$$R(\rho_t, u_t) = -\frac{1}{2} \int_{\Omega} |u_t|^2 \rho_t dx - \gamma \int_{\Omega} \int_{\Omega} \frac{\rho_t(y) \rho_t(x)}{a(x, y)} dy dx, \quad (97)$$

where $a(x, y) := 0.1 + |y - x|^2$ is the agent interaction (repelling) term that imposes penalty if two agents are too close which may lead to collision. We set the terminal reward function $g(x) = -|x|^2/2$ and the terminal time $T = 1$, which encourages the agents to gather at the target point 0 at $T = 1$. The initial density is set to $p(x) = \mathcal{N}(x; -2\mathbf{1}_d, 0.5I_d)$, which is a Gaussian with mean $-2\mathbf{1}_d$ and covariance $0.5I_d$. Here $\mathbf{1}_d$ denotes the d -dimensional vector with all components equal to 1. We test Algorithm 1 to solve the optimal probability control problem (7) without and with the interaction term in (97) by setting $\gamma = 0$ and $\gamma = 5$, respectively.

The resulting agent distributions at times $t = 0, 0.25, 0.5, 0.75$, and 1 are shown with different colors at different dimension sections in Figure 1. In the top row of Figure 1, we observe the expected agent movements along time and tendency to avoid collision when $\gamma = 5$. In the bottom row of Figure 1, we turn off the interaction term by setting $\gamma = 0$, and observe that the agents tend to clump together as they approach the target point 0.

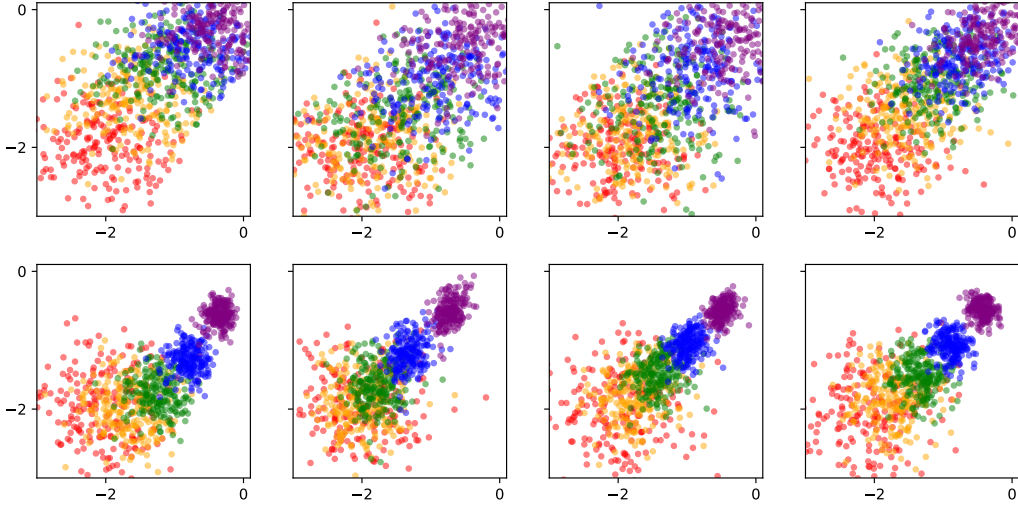


Figure 1: (Test 1) Visualization of agent movements under u solved by Algorithm 1 for the probability control problem with running reward (97). Agent distributions are shown by colored circles at different times $t = 0$ (red), 0.25 (orange), 0.5 (green), 0.75 (blue), and 1 (purple). Top row and bottom row show the results with and without agent collision preventions, i.e., $\gamma = 5$ and $\gamma = 0$, respectively. The plots from left to right columns show the agent distributions in the (x_1, x_2) , (x_3, x_4) , (x_5, x_6) , and (x_7, x_8) coordinates, respectively.

5.2 Test 2 with Regional Obstacle

We consider the probability control problem (7) where the goal is to move the agents close to a specified location x^* without hitting on a fixed obstacle in Ω . We set $\Omega = \mathbb{R}^d$ with $d = 30$ and $d = 100$, and in each case we place a cylindrical obstacle of radius 0.5 with $\{(0, 0, x_3, \dots, x_d) : x_i \in \mathbb{R}, i = 3, \dots, d\}$ as the center line. We define

$$b(x) = \begin{cases} (x_1^2 + x_2^2) - \frac{1}{4}, & \text{if } x_1^2 + x_2^2 > \frac{1}{4}, \\ 0, & \text{elsewhere,} \end{cases}$$

which is 0 if x is in the obstacle, and becomes larger as x gets further away from the obstacle. The running reward is set to

$$R(\rho_t, u_t) = -\frac{1}{2} \int |u_t|^2 \rho_t dx - \int \frac{1}{\epsilon + b(x)} \rho_t(x) dx, \quad (98)$$

where $\epsilon = 0.1$ is used for computation stability.

We set the terminal time $T = 1$ and the terminal reward functional to

$$G(q) = - \int_{\Omega} |x - x^*|^2 q(x) dx \quad (99)$$

where $x^*(1, -0.5, 0, \dots, 0) \in \mathbb{R}^d$ is the target spot where the agents should get around at terminal time.

We set the initial probability density to

$$p(x) = \chi\left(x_1 + \frac{1}{2}\right) e^{x_1 + \frac{1}{2}} \mathcal{N}(x_{2:d}; (0.5, 0, \dots, 0), 0.25I_{d-1})$$

where $x_{2:d} := (x_2, \dots, x_d)$ and $\chi(z) = 1$ if $z \leq 0$ and 0 otherwise. Therefore, the agents are close to but not inside the obstacle at the initial time $t = 0$.

We solve the optimal probability control problem (7) with the setting above for $d = 30$ and $d = 100$, and plot the results in Figure 2. Figure 2 shows the agent distributions at different time spots $t = 0, 0.25, 0.5, 0.75$, and 1 in the (x_1, x_2) coordinates for domain dimension $d = 30$ (left plot) and $d = 100$ (right plot).

In both plots in Figure 2, we see the control vector field u obtained by Algorithm 1 can successfully steer the agents around the obstacle to reach the target location x^* . Note that the result demonstrates that the proposed Algorithm 1 is scalable to cases where dimension d can be as high as 100.

5.3 Test 3 with Squeezing Obstacle and Agent Interaction

In this experiment, we consider the control problem with both agent interaction and an obstacle. We set $\Omega = \mathbb{R}^d$ where $d = 30$. We place a squeezing obstacle which is formed by two wedges, and the agents need to move from their original locations to the target location $x^* = (2, 0, \dots, 0) \in \mathbb{R}^d$ by passing through the gate between the two wedges.. The shape of the wedge and the agent locations in the (x_1, x_2) coordinates are shown in Figure 3.

In this test, we define

$$b(x) = \begin{cases} 50(5x_1^2 - x_2^2 - 0.1), & \text{if } 5x_1^2 - x_2^2 + 0.1 \geq 0, \\ 0, & \text{elsewhere.} \end{cases}$$

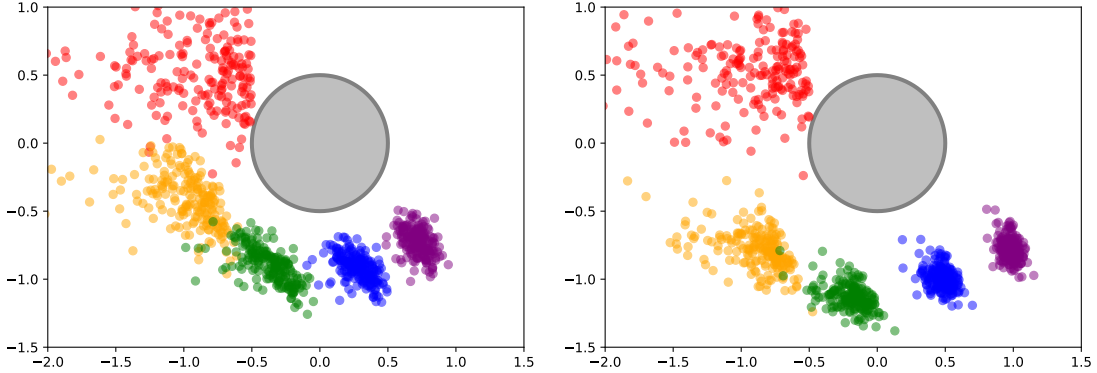


Figure 2: (Test 2) Visualization of agent movements under u solved by Algorithm 1 for the probability control problem with cylindrical obstacle (98). Agent distributions are shown by colored circles at different times $t = 0$ (red), 0.25 (orange), 0.5 (green), 0.75 (blue), and 1 (purple). The plots show the agent distributions in the (x_1, x_2) coordinates for dimensions $d = 30$ (left plot) and $d = 100$ (right plot).

We set the running reward functional R as (98), and also add an interaction term identical to the second term on the right-hand side of (97) with penalty weight γ . We use the same terminal reward functional G as in Test 2 with x^* chosen as above. We choose an initial density $p(x) = \mathcal{N}(x; (-2, 0, \dots, 0), 0.5I_d)$ and again set the terminal time to $T = 1$. The results for the cases without this interaction ($\gamma = 0$) and with this interaction ($\gamma = 1$) are shown in the left and right plots, respectively, in Figure 3.

We observe that the agents can squeeze through the gate between the two wedges in both plots of Figure 3, and larger γ causes the agents to keep distances from each other when they move. In particular, they slowly start spreading out again as they exit the gate when $\gamma = 1$, as shown in the right plot.

6 Conclusion

In this paper, we present a comprehensive theoretical framework of optimal probability density control in the standard measure spaces. Specifically, we establish two fundamental results in this setting: the maximum principle of optimal control vector fields and the Hamilton–Jacobi–Bellman equation of value functional. The results are concise, easy to interpret, and supported by rigorous mathematical analysis. This new framework does not require Wasserstein metrics typically used in the literature. This allows substantial simplifications of numerical computations in practice. We present a scalable algorithm aligned with the maximum principle and demonstrate its promising performance on several high-dimensional multi-agent control problems.

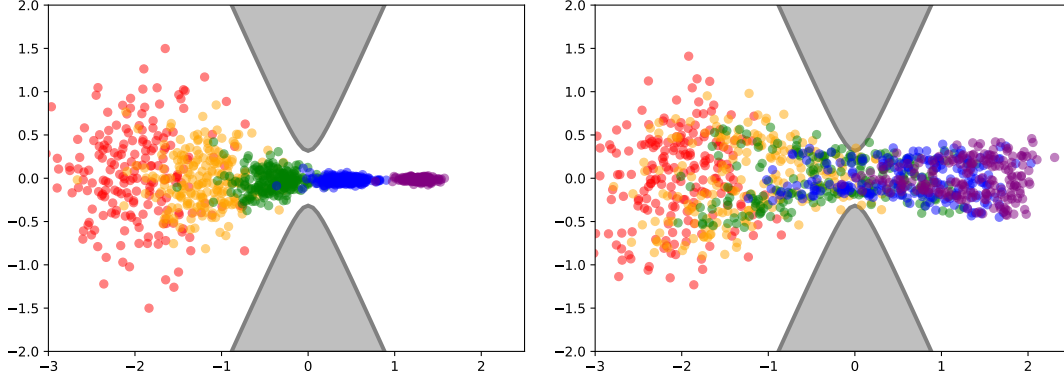


Figure 3: (Test 3) Visualization of agent movements under u solved by Algorithm 1 for the probability control problem with both wedge obstacles and agent interaction. Agent distributions are shown by colored circles at different times $t = 0$ (red), 0.25 (orange), 0.5 (green), 0.75 (blue), and 1 (purple). The plots show the agent distributions in the (x_1, x_2) coordinates with penalty weight $\gamma = 0$ (left plot) and $\gamma = 1$ (right plot) of the interaction term.

References

- [1] L. Ambrosio, L. A. Caffarelli, Y. Brenier, G. Buttazzo, and C. Villani. *Optimal transportation and applications*, volume 1813 of *Lecture Notes in Mathematics*. Springer-Verlag, Berlin, 2003.
- [2] L. Ambrosio and W. Gangbo. Hamiltonian ODEs in the wasserstein space of probability measures. *Communications on Pure and Applied Mathematics: A Journal Issued by the Courant Institute of Mathematical Sciences*, 61(1):18–53, 2008.
- [3] L. Ambrosio and N. Gigli. A users guide to optimal transport. In *Modelling and Optimisation of Flows on Networks*, pages 1–155. Springer, 2013.
- [4] M. Bongini, M. Fornasier, F. Rossi, and F. Solombrino. Mean-field pontryagin maximum principle. *Journal of Optimization Theory and Applications*, 175:1–38, 2017.
- [5] J. F. Bonnans. On an algorithm for optimal control using pontryagin’s maximum principle. *SIAM Journal on Control and Optimization*, 24(3):579–588, 1986.
- [6] B. Bonnet. A pontryagin maximum principle in wasserstein spaces for constrained optimal control problems. *ESAIM: Control, Optimisation and Calculus of Variations*, 25:52, 2019.
- [7] B. Bonnet and H. Frankowska. Necessary optimality conditions for optimal control problems in wasserstein spaces. *Applied Mathematics & Optimization*, 84(2):1281–1330, 2021.
- [8] B. Bonnet and F. Rossi. The pontryagin maximum principle in the wasserstein space. *Calculus of Variations and Partial Differential Equations*, 58(1):11, 2019.

- [9] M. Brambilla, E. Ferrante, M. Birattari, and M. Dorigo. Swarm robotics: a review from the swarm engineering perspective. *Swarm Intelligence*, 7:1–41, 2013.
- [10] T. Breitenbach and A. Borzi. The pontryagin maximum principle for solving fokker–planck optimal control problems. *Computational Optimization and Applications*, 76(2):499–533, 2020.
- [11] P. E. Caines, M. Huang, and R. P. Malhamé. Large population stochastic dynamic games: closed-loop mckean-vlasov systems and the nash certainty equivalence principle. *Communications in Information and Systems*, 6(3):221–252, 2006.
- [12] R. T. Chen, Y. Rubanova, J. Bettencourt, and D. K. Duvenaud. Neural ordinary differential equations. *Advances in neural information processing systems*, 31, 2018.
- [13] L. Dinh, D. Krueger, and Y. Bengio. Nice: Non-linear independent components estimation. *arXiv preprint arXiv:1410.8516*, 2014.
- [14] M. Dorigo, G. Theraulaz, and V. Trianni. Swarm robotics: Past, present, and future [point of view]. *Proceedings of the IEEE*, 109(7):1152–1165, 2021.
- [15] Y. Du and T. A. Zaki. Evolutional deep neural network. *Physical Review E*, 104(4):045303, 2021.
- [16] M. Duprez, M. Morancey, and F. Rossi. Approximate and exact controllability of the continuity equation with a localized vector field. *SIAM Journal on Control and Optimization*, 57(2):1284–1311, 2019.
- [17] U. Eren and B. Açıkmeşe. Velocity field generation for density control of swarms using heat equation and smoothing kernels. *IFAC-PapersOnLine*, 50(1):9405–9411, 2017.
- [18] Z. Feng, G. Hu, Y. Sun, and J. Soon. An overview of collaborative robotic manipulation in multi-robot systems. *Annual Reviews in Control*, 49:113–127, 2020.
- [19] M. Fornasier, S. Lisini, C. Orrieri, and G. Savaré. Mean-field optimal control as gamma-limit of finite agent controls. *European Journal of Applied Mathematics*, 30(6):1153–1186, 2019.
- [20] M. Fornasier and F. Solombrino. Mean-field optimal control. *ESAIM: COCV*, 20(4):1123–1152, 2014.
- [21] K. Hoshino. Finite-horizon control of nonlinear discrete-time systems with terminal cost of wasserstein distance. In *2020 59th IEEE Conference on Decision and Control (CDC)*, pages 4268–4274. IEEE, 2020.
- [22] K. Hoshino. Finite-horizon optimal control of continuous-time stochastic systems with terminal cost of wasserstein distance. In *2023 62nd IEEE Conference on Decision and Control (CDC)*, pages 5825–5830. IEEE, 2023.
- [23] D. Inoue, Y. Ito, and H. Yoshida. Optimal transport-based coverage control for swarm robot systems: Generalization of the voronoi tessellation-based method. In *2021 American Control Conference (ACC)*, pages 3032–3037. IEEE, 2021.

- [24] F. Jean, O. Jerhaoui, and H. Zidani. A mayer optimal control problem on wasserstein spaces over riemannian manifolds. *IFAC-PapersOnLine*, 55(16):44–49, 2022.
- [25] C. Jimenez, A. Marigonda, and M. Quincampoix. Optimal control of multiagent systems in the wasserstein space. *Calculus of Variations and Partial Differential Equations*, 59(2):58, 2020.
- [26] D. P. Kingma and J. Ba. Adam: A method for stochastic optimization. In Y. Bengio and Y. LeCun, editors, *3rd International Conference on Learning Representations, ICLR 2015, San Diego, CA, USA, May 7-9, 2015, Conference Track Proceedings*, 2015.
- [27] J.-M. Lasry and P.-L. Lions. Mean field games. *Japanese journal of mathematics*, 2(1):229–260, 2007.
- [28] S. Ma, M. Hou, X. Ye, and H. Zhou. High-dimensional optimal density control with wasserstein metric matching. In *2023 62nd IEEE Conference on Decision and Control (CDC)*, pages 6813–6818. IEEE, 2023.
- [29] H. P. McKean. Propagation of chaos for a class of non-linear parabolic equations. *Stochastic Differential Equations (Lecture Series in Differential Equations, Session 7, Catholic Univ., 1967)*, pages 41–57, 1967.
- [30] M. Nourian and P. E. Caines. ϵ -Nash mean field game theory for nonlinear stochastic dynamical systems with major and minor agents. *SIAM Journal on Control and Optimization*, 51(4):3302–3331, 2013.
- [31] N. Pogodaev. Numerical algorithm for optimal control of continuity equations. In *CEUR Workshop Proceedings*, pages 467–474, 2017.
- [32] M. Raissi, P. Perdikaris, and G. E. Karniadakis. Physics-informed neural networks: A deep learning framework for solving forward and inverse problems involving nonlinear partial differential equations. *Journal of Computational Physics*, 378:686–707, 2019.
- [33] S. Roy, M. Annunziato, A. Borzi, and C. Klingenberg. A fokker–planck approach to control collective motion. *Computational Optimization and Applications*, 69:423–459, 2018.
- [34] Y. Sakawa and Y. Shindo. On global convergence of an algorithm for optimal control. *IEEE Transactions on Automatic Control*, 25(6):1149–1153, 1980.
- [35] C. Sinigaglia, A. Manzoni, and F. Braghin. Density control of large-scale particles swarm through pde-constrained optimization. *IEEE Transactions on Robotics*, 38(6):3530–3549, 2022.
- [36] C. Villani. *Topics in Optimal Transportation*. American Mathematical Society, 2003.
- [37] C. Villani. *Optimal transport: old and new*, volume 338. Springer Science & Business Media, 2008.